IL-27 enhances the lymphocyte mediated innate resistance to primary hookworm infection in the lungs

Jason B. Noon [§,*], Arjun Sharma[§, †, *], Johannes Platten[†], Lee J. Quinton[§], Christoph Reinhardt[†], and Markus Bosmann[§, †, ‡]

[§]Pulmonary Center, Department of Medicine, Boston University School of Medicine, Boston, Massachusetts, 02118, USA

[†]Center for Thrombosis and Hemostasis, University Medical Center of the Johannes Gutenberg University Mainz, 55131, Mainz, Germany

[‡]Research Center for Immunotherapy (FZI), University Medical Center of the Johannes Gutenberg-University Mainz, 55131, Mainz, Germany

[*]These authors contributed equally to the work.

Corresponding Author: Markus Bosmann, Associate Professor of Medicine, Pathology & Laboratory Medicine, Pulmonary Center, Department of Medicine, Boston University School of Medicine, Boston, Massachusetts, 02118, USA, Phone: +1-617-358-1225, FAX: +1-617-638-5227. E-mail: mbosmann@bu.edu

Key words: Inflammation, parasitic-helminth, cytokines, rodent, immunology

Total word count: 5252 words

Content type: Article

Abstract

Interleukin-27 (IL-27) is a heterodimeric cytokine of the IL-12 family, formed by non-covalent association of the promiscuous EBI3 subunit and selective p28 subunit. IL-27 is produced by mononuclear phagocytes and unfolds pleiotropic immune-modulatory functions through high affinity ligation to IL-27 receptor alpha (IL-27RA). While IL-27 is known to contribute to immunity and to end inflammation following numerous types of infections, its relevance for host defense against multicellular parasites is still poorly defined. Here, we investigated the role of IL-27 during infection with the soil-transmitted hookworm, *Nippostrongylus brasiliensis*, in its early intrapulmonary life cycle. IL-27(p28) was detectable in broncho-alveolar lavage fluids of C57BL/6J wild type mice on day 1 after subcutaneous *N. brasiliensis* inoculation. The expression of IL-27RA was most abundant on lung invading γδ T cells followed by $CD8^+$ T cells, $CD4^+$ T cells and NK cells. IL-27RA was weakly present on $CD19^+$ B cells and absent on neutrophils, alveolar macrophages and eosinophils. $Il27ra^{-/-}$ mice showed increased parasite burden together with aggravated pulmonary hemorrhage and higher alveolar albumin leakage as a surrogate for disruption of the epithelial/vascular barrier. Conversely, recombinant mouse IL-27 injections of wild type mice reduced parasite burdens and lung injury. In multiplex screens, we identified higher airway accumulations of IL-6, TNFα and MCP-3 (CCL7) in $Il27ra^{-/-}$ mice, while rmIL-27 treatment showed a reciprocal effect. Finally, γδ T cell infiltration of the airways required endogenous IL-27 expression. In summary, this report demonstrates protective functions of IL-27 to control the early larval stage of hookworm infection in the lungs.

Introduction

Hookworms are soil-transmitted intestinal nematodes that have a critical stage in development within the airspaces of the lungs (1). After molting from an infectious third stage (L3) to an L4 stage within the alveolar space, hookworms ascend the trachea and are swallowed, ultimately infecting the small intestine where they remain as egg-laying adults. In the small intestine, hookworms rupture vessels and feed on blood, which is the cause of clinical hookworm disease characterized by iron-deficiency anemia. Over 500 million people worldwide are infected with hookworms (2, 3), and among all parasites, hookworms are behind only malaria for the leading causes of iron-deficiency anemia globally (4-7), indicating the importance of these parasites. Although there are anthelmintic drugs available for treating hookworms (8, 9), people are rapidly re-infected in endemic areas due to insufficient immunity and high vulnerability for secondary infections (10). Importantly, there is not a single licensed hookworm vaccine (11), stressing the value of understanding protective immunity to hookworm infections.

Murine hookworm *Nippostrongylus brasiliensis* is a model for human hookworm disease, particularly for the stage of infection within the lungs, which occurs on days 1 and 2 after subcutaneous inoculation (12). On day 3, larvae transition to the small intestine and remain until day 7. There are many publications that indicate the importance of the canonical type 2 response involving cytokines such as IL-4, IL-5, IL-13 and RELMβ, along with group 2 innate lymphoid cells (ILC2s), type 2 T helper (Th2) cells, alternatively activated macrophages, eosinophils, basophils, mast cells and goblet cells in resistance to secondary *N. brasiliensis* infections in the lungs (13), which does not occur in humans. However, knowledge on primary *N. brasiliensis* infection in the lungs is sparse (14, 15). Resistance to primary hookworm infections (in animals) is widely believed to be localized to the small intestine stage of infection and, in the *N. brasiliensis*

model, is well-characterized by canonical type 2-driven expulsion mediated by ILC2s and Th2 cells (13), as well as type 2 γδ T (γδ T2) cells (i.e., intestinal intraepithelial T lymphocytes; IELs) (16). Although much less is known about primary resistance in the lungs to hookworm infections, in the *N. brasiliensis* model, IL-17A, neutrophils and γδ T cells (14), and interestingly, ILC2s (15) are involved.

IL-27 is a heterodimeric cytokine composed of a unique p28 α-subunit and an EBI3 β-subunit (17). EBI3 is shared with IL-35 (18). The IL-27 receptor is also a heterodimer composed of a unique IL-27 receptor α-subunit (IL-27RA, WSX-1) and a gp130 β-subunit that is shared with multiple other cytokine receptors (17, 19, 20). IL-27 is well-described to exert acute pro-inflammatory effects, enhancing type 1 responses, particularly $CD8^+$ cytotoxic lymphocytes (CTLs) and natural killer (NK) cells, thus enhancing protective immunity to intracellular pathogens and various cancers (21). Consistent with IL-27 enhancing type 1 responses, IL-27 directly suppresses the expansion and activation of ILC2s during the lung repair phase of primary *N. brasiliensis* infections (22). A more rapid intestinal expulsion is seen in the absence of IL-27 activities in both models of hookworm (studying $Ebi3^{-/-}$ mice) and whipworm (studying $Il27ra^{-/-}$ mice) infections (22, 23). Importantly, there are no publications on IL-27 during early primary *N. brasiliensis* infections in the lungs, or any other helminth infection. As ILC2s are involved in limiting primary *N. brasiliensis* infections in the lungs (24, 25) and IL-27 antagonizes tissue-resident ILC2s (26), we initially hypothesized that IL-27 limits resistance to primary *N. brasiliensis* infections in the lungs by suppressing type 2 responses. Interestingly, however, we found that IL-27 enhances resistance to primary *N. brasiliensis* infections in the lung alveolar space in association with increased expansion of γδ T cells, which we also found to express much higher levels of IL-27RA compared both $CD4^+$ Th cells and $CD8^+$ CTLs.

In conclusion, future efforts for the development of a hookworm vaccine may be inspired by the concept of targeting the lung larval stage and considering adjuvants likely to induce strong IL-27-dependent immunity (11, 27-29).

Materials and Methods

Mice

All procedures with mice were approved by the Institutional Animal Care and Use Committee of the Boston University and performed in compliance with the guidelines of the National Institutes of Health. IL-27RA$^{-/-}$ mice (B6N.129P2-Il27ra^{tm1Mak}/J; on C57BL/6NJ background), C57BL/6NJ mice and C57BL/6J mice were obtained from the Jackson Laboratory (Bar Harbor, ME). The mice were bred and genotyped at the animal facilities of the Boston University under specific pathogen-free conditions and controlled light/dark cycle. Male and female mice at 8-12 weeks of age were used for experiments.

Nippostrongylus brasiliensis cultures and inoculations

N. brasiliensis coprocultures were provided by Dr. Joseph Urban Jr., United States Department of Agriculture. L3 were extracted from coprocultures and prepared for inoculations according to an established protocol (12). Mice were injected subcutaneously in the flank with 500 L3 in 0.1 mL of sterile PBS (Thermo Fisher Scientific, Waltham, MA).

Alveolar and lung tissue parasite burdens

To measure alveolar parasite burden, inoculated mice were euthanized by CO_2 overdose, and three bronchoalveolar lavages (BAL) were collected before vital organ removal. For the first BAL, 1

mL PBS containing 1X HALT Protease Inhibitor Cocktail/EDTA (Thermo Fisher Scientific) was collected into a 1.5 mL tube. PBS only was used for the second and third BAL and were collected into a 50 mL tube on ice. The first BAL was centrifuged at 400 x g for 8 min at room temperature and the cell-free supernatant was collected as BAL fluid (BALF) and stored at -80°C for later analysis. The pellet of BAL cells and containing *N. brasiliensis* larvae was then resuspended in PBS and transferred to the 50 mL tube along with the additional BAL collections. The combined BAL was then diluted to 30 mL with PBS and transferred to a 100 mm petri dish with grids drawn on the bottom surface. All intact *N. brasiliensis* larvae were counted under 20X magnification (AmScope, Irvine, CA), excluding *N. brasiliensis* debris and obviously dead and deteriorating larvae. The suspension of BAL cells and *N. brasiliensis* larvae was then transferred back to the 50 mL tube and centrifuged at 800 x g for 8 min at 4°C. The supernatant was removed down to 10 mL, then the BAL cell pellet was resuspended, transferred to a 15 mL tube and centrifuged as before. The supernatant was removed down to 0.5 mL, then the BAL cell pellet was transferred to a 1.5 mL tube before further analysis. To measure parasite burden in lung tissues, lungs were collected from inoculated mice after BAL collections into 35 mm petri dishes. Lungs were minced with a surgical scissors, resuspended in 5 mL of a 37°C slurry of 1% agarose, and then pipetted onto a flattened layer of cheesecloth. Once solidified, the cheesecloth was rolled up and placed in a submerging vessel of 45 mL PBS in a 50 mL tube, with a small piece of the cheesecloth secured between the tube and lid, and then incubated in 37°C overnight. Larvae that migrated out of the lung tissues and agarose were counted under 20X magnification.

Alveolar injury

BALF total protein was measured with a Pierce BCA Protein Assay Kit (Thermo Scientific). Alveolar hemorrhage was assessed as described elsewhere (30), but with the following modifications. A 6X 2-fold serial dilution (8000-250 µg/mL) of human hemoglobin (Sigma, St. Louis, MO) was prepared, and 50 µL of each standard and BAL sample was added to duplicate wells of a 96-well plate. A volume of 100 µL of 6% sodium dodecyl sulfate (Sigma) was added to all wells and resuspended several times. The absorbance at 560 nm was measured with a Tecan Infinite M Nano plate reader (Tecan, Männedorf, Switzerland), and alveolar hemorrhage (i.e., total amount of hemoglobin recovered in BAL) was determined from the standard curve generated by Magellan V 7.2 (Tecan) software.

ELISA & multiplex bead-based immunoassay

IL-27(p28) in BALF was measured with a mouse IL-27 p28/IL-30 DuoSet ELISA (R&D Systems, Minneapolis, MN), according to the manufacturer's instructions. The absorbance at 450 nm was measured with a Tecan Infinite M Nano plate reader, and concentration was determined from the standard curve generated by Magellan software.

A multiplex bead-based immunoassay (Cytokine & Chemokine 26-Plex Mouse ProcartaPlex™ Panel 1, Thermo Fisher Scientific) was used for simultaneous quantification of the following cytokines/chemokines: IL-1β, IL-2, IL-4, IL-5, IL-6, IL-9, IL-10, IL-12p70, IL-13, IL-17A, IL-18, IL-22, IL-23, IL-27, GROα (CXCL-1), IP-10 (CXCL-10), MCP-1 (CCL-2), MCP-3 (CCL-7), MIP-1α (CCL-3), MIP-1β (CCL-4), MIP-2 (CXCL-2), RANTES (CCL-5), Eotaxin (CCL-11), GM-CSF, IFN gamma, and TNF alpha (31). All samples from bead-based assays were performed using a LiquiChip-200 instrument (Qiagen, Hilden, Germany) using Bio-Plex Manager v6.1 software for quantification.

157

158 *Flow Cytometry*

159 Fresh BAL cells were collected from inoculated mice as described above. In multiple experiments
160 using our standard operating procedures, >99% of BAL cells were found to be negative for fixable
161 viability dye eFlour 780 (eBioscience, ThermoFisher Scientific), and hence, all BAL cells are
162 considered alive. BAL cells collected in a 15 mL tube were centrifuged 800 x g at 4°C for 8 min,
163 and then resuspended in the following mouse antibody staining cocktails, transferred to 1.5 mL
164 tubes, and then incubated in the dark for 30 min at 4°C: Myeloid-lymphocyte common lineage
165 panel – TruStain FcX (anti-CD16/32) (clone: 93; dilution: 1:100, BioLegend, San Diego, CA),
166 CD45-Pacific Blue (clone: 30-F11; dilution 1:200, BioLegend), Ly6G-APC (clone: 1A8; dilution:
167 1:400, BioLegend), Siglec-F-APC/Cy7 (clone: E50-2440; dilution: 1:200, BioLegend), CD11c-
168 Alexa Fluor 488 (clone: N418; dilution: 1:600, BioLegend), CD3-BUV737 (clone: 145-2C11;
169 dilution: 1:100, BD Biosciences, San Jose, CA), CD19-PE/Cy7 (clone: 6D5; dilution: 1:100,
170 BioLegend), NK1.1-PerCP/Cy5.5 (clone: PK136; dilution: 1:100, BioLegend), IL-27RA-PE
171 (clone: 2918; dilution: 1:100, BD Biosciences); T cell panel – TruStain FcX (anti-CD16/32)
172 (clone: 93; dilution: 1:100, BioLegend), CD3-BUV737 (clone: 145-2C11; dilution: 1:100, BD
173 Biosciences), TCRβ chain-PE/Cy7 (clone: H57-597; dilution: 1:100, BioLegend), CD4-Alexa
174 Fluor 488 (clone: RM4-5; dilution 1:400, BioLegend), CD8a-APC/Cy7 (clone: 53-6.7; dilution:
175 1:100, BioLegend), TCRγδ-APC (clone: GL3; dilution: 1:00, BioLegend), NK1.1-PerCP/Cy5.5
176 (clone: PK136; dilution: 1:100, BioLegend), IL-27RA-PE (clone: 2918; dilution: 1:100, BD
177 Biosciences) or PE Rat IgG2a, κ Isotype Control (clone: R35-95; dilution: 1:100, BD Biosciences).
178 All antibodies were diluted in FACS buffer prepared from sterile PBS and supplemented with
179 0.25% (w/v) BSA, 0.02% (w/v) sodium azide and 2 mM EDTA. The stained cells were rinsed in

FACS buffer, and then fixed in 2% paraformaldehyde (Santa Cruz Biotechnology, Dallas, TX) at room temperature for 20 min. Stained/fixed cells were centrifuged as described before, resuspended in FACS buffer and transferred to a FACS tube containing 20 µL of CountBright Absolute Counting Beads (ThermoFisher Scientific). For all single-stained compensation controls, we used OneComp eBeads Compensation Beads (Invitrogen) according to the manufacturer's instructions. Flow cytometric analysis was performed on a BD LSR II flow cytometer with BD FACSDiva software. Final plots were made in FlowJo v10.

Reagents

Recombinant mouse IL-27 (<1.0 EU per 1 µg of the rmIL-27 protein by the LAL method) was purchased from R&D systems.

Data analysis

Statistical analyses were performed and graphs were prepared in Prism v7.04-v8.4.3 (GraphPad Software). Data in bar graphs are depicted as mean ± standard error of the mean (S.E.M.), with overlaid symbols representing values from individual mice. Two-group single comparisons were made with a t-test (with parametric data pre-confirmed using the F test). Multiple comparisons were made with a one-way ANOVA followed by Tukey's post hoc test. *P* values <0.05 were considered significant. *P* values <0.1 were considered as a trend.

Results

IL-27(p28) is transiently elevated in alveolar space during primary N. brasiliensis infection of the lungs

While *N. brasiliensis* infection is well known, to induce an eosinophilic and Th2 cell dependent immune response, the role of the immune-modulatory cytokine IL-27 is not well described in the pulmonary state of the hookworm infection cycle. To test if IL-27(p28) is released during primary *N. brasiliensis* infection of the lungs, C57BL/6J mice (wild type, WT) were inoculated with n=500 *N. brasiliensis* L3, and EDTA-plasma was collected on days 0, 1, 2, 6 and 9 following infection. BALF was collected on days 0, 1, 2 and 9 post infection (p.i.). Circulating IL-27(p28) was not detectable in EDTA-plasma by ELISA at any of the studied time points, even though all mice were confirmed to be highly infected with an average of 40,000 eggs per gram of feces on day 6 p.i. (data not shown). However, in BALF, IL-27(p28) was elevated by ~2.6-fold on day 1 p.i. compared to day 0 ($P<0.0001$, Fig. 1). The concentrations of IL-27(p28) returned to normal levels by day 2 (Fig. 1). Thus, these results indicate that IL-27(p28) is transiently released specifically in the alveolar space during primary *N. brasiliensis* infection of the lungs. The bulk of IL-27 may avidly bind to its receptor for rapid clearance or altogether escape detection in cell-free BALF.

IL-27RA is highly expressed on T cells in alveolar space during primary pulmonary N. brasiliensis infection

To study if IL-27RA is expressed on invading immune cells in the broncho-alveolar space during primary *N. brasiliensis* infection of the lungs, we first confirmed leukocyte dynamics in BAL from C57BL/6J mice on days 0, 1 and 2 p.i. with *N. brasiliensis* larvae. Within the myeloid lineage, we recovered an average of ~70,000 $CD11c^{+}Siglec\text{-}F^{+}$ resident alveolar macrophages per mouse in

BAL on day 0 in sham mice (Fig. S1A, S1B). The numbers of alveolar macrophages were similar in BAL on day 1 p.i., while recovery of this cell type increased to ~120,000 in BAL by day 2 p.i. (Fig. S1A, S1B). In addition, while no $Ly6G^+$ neutrophils or $CD11c^-$Siglec-F^+ eosinophils were present in BAL of sham mice, the numbers of these myeloid cells substantially increased over the course of 2 days following *N. brasiliensis* infection (Fig. S1B). Furthermore, within the lymphocyte lineage, while few cells were detectable in day 0 p.i. BAL, accumulation of $CD19^+CD3^-$ B cells, $CD19^-CD3^+$ T cells and $CD19^-CD3^-NK1.1^+$ NK cells was detected on day 1 and further elevated on day 2 (Fig. 2A, 2B). Thus, all investigated myeloid and lymphoid cells increase in the alveolar space during the natural course of primary *N. brasiliensis* infection.

Essentially none of the three myeloid cell types (neutrophils, eosinophils, alveolar macrophages) present in BAL after infection were found to express IL-27RA at any time point evaluated (Fig. S1C). However, an average of 80.2%, 56.1% and 23.1% of $CD19^-CD3^+$ T cells, $CD19^-CD3^-NK1.1^+$ NK cells and $CD19^+CD3^-$ B cells were IL-$27RA^+$, and these percentages were similar on both day 1 and 2 p.i. (Fig. 2C, 2D). Geometric mean fluorescence intensities (gMFI) of IL-27RA were 2-fold greater on $CD19^-CD3^+$ T cells on day 2 compared to day 1 p.i. (suggesting T cell-specific upregulation of IL-27RA, Fig. 2E), while IL-27RA gMFI was similar on $CD19^-CD3^-NK1.1^+$ NK cells and $CD19^+CD3^-$ B cells at the two time points studied (Fig. 2E). Moreover, IL-27RA gMFI was >3-fold higher on $CD19^-CD3^+$ T cells compared to $CD19^-CD3^-NK1.1^+$ NK cells and $CD19^+CD3^-$ B cells. Hence, the frequency and magnitude of IL-27RA expression is greatest on $CD19^-CD3^+$ T cells in the alveolar space during primary *N. brasiliensis* infection of the lungs.

We next evaluated the numbers of different T cell subsets in the alveolar space during primary pulmonary *N. brasiliensis* infection, and for their expression of IL-27RA. Both

246 TCRβ$^+$CD4$^+$ Th cells and TCRβ$^+$CD8$^+$ CTLs became considerably more abundant than TCRβ$^-$
247 TCRγδ$^+$ γδ T cells after *N. brasiliensis* infection, while none of these lymphocyte populations were
248 present in BAL from uninfected mice (Fig. 3A, 3B). The numbers of TCRβ$^+$CD4$^+$ Th cells,
249 TCRβ$^+$CD8$^+$ CTLs and TCRβ$^-$TCRγδ$^+$ γδ T cells further increased from day 1 to day 2 (Fig. 3A,
250 3B). Moreover, >40% of all three subsets were IL-27RA$^+$ (Fig. 3C, 3D). There was a significantly
251 higher percentage of IL-27RA$^+$TCRβ$^-$TCRγδ$^+$ γδ T cells compared to IL-27RA$^+$TCRβ$^+$CD8$^+$
252 CTLs and IL-27RA$^+$TCRβ$^+$CD4$^+$ Th cells, while there was not a significant difference between
253 IL-27RA$^+$TCRβ$^+$CD8$^+$ CTLs and IL-27RA$^+$TCRβ$^+$CD4$^+$ Th cells (Fig. 3D). Furthermore, TCRβ$^-$
254 TCRγδ$^+$ γδ T cells resulted in significantly higher IL-27RA gMFI compared to both TCRβ$^+$CD8$^+$
255 CTLs and TCRβ$^+$CD4$^+$ Th cells, and TCRβ$^+$CD8$^+$ CTLs resulted in significantly higher IL-27RA
256 gMFI compared to TCRβ$^+$CD4$^+$ Th cells (Fig. 3E). Thus, IL-27RA is most prevalent and most
257 highly expressed on γδ T cells, but Th cells and CTLs dominate the T cell population in the alveolar
258 space during primary *N. brasiliensis* infection of the lungs.
259
260 *IL-27 signaling enhances resistance to primary N. brasiliensis infections in the lungs*
261 To determine if IL-27 has a beneficial or detrimental role during primary *N. brasiliensis* infection
262 of the lungs, we first inoculated Il27ra$^{-/-}$ mice and C57BL/6NJ wild type (WT) mice with 500 *N.*
263 *brasiliensis* L3 and compared alveolar parasite burden, hemorrhage and total protein on day 2 p.i..
264 Strikingly, Il27ra$^{-/-}$ mice showed a 2.2-fold increase in alveolar parasite burdens compared to WT
265 mice (Fig. 4A). We confirmed that the majority of parasites are recovered by the BAL procedure
266 with only few remaining larvae in lung tissues (Fig. S2). To evaluate the severity of parasite-
267 induced lung injury, we determined hemoglobin concentrations in BAL as a marker for airway
268 hemorrhage and broncho-alveolar albumin as a surrogate endpoint for the disturbance of the

epithelial/vascular barrier function. A significant 1.9-fold increase in alveolar hemorrhage in Il27ra$^{-/-}$ mice compared to WT mice was observed in line with the greater parasite burden of Il27ra$^{-/-}$ mice (Fig. 4B). Moreover, and also consistent with the greater parasite burden, a moderate but significant 1.3-fold increase in total protein leakage was detected in the BALF of Il27ra$^{-/-}$ mice (Fig. 4C), indicating an increase in proteinaceous edema.

Next, we tested whether administration of exogenous IL-27 would further reduce the severity of *N. brasiliensis* infection in the lungs of WT mice. Therefore, we administered 100 ng recombinant mouse IL-27 (rmIL-27) intraperitoneally on days 0 and 1 p.i. in C57BL/6J mice and compared alveolar parasite burden and injury with a carrier/mock alone group. The rmIL-27 treatment significantly reduced the alveolar parasite burden to 65% of mock controls (Fig. 4D). In addition, alveolar hemorrhage was significantly decreased to 72% of mock controls (Fig. 4E), while there was a slight, albeit statistically insignificant, decrease in total alveolar protein leakage (Fig. 4F). Taken together, these results indicate that both endogenous IL-27/IL-27RA signaling and therapeutic recombinant IL-27 enhance the innate resistance to primary *N. brasiliensis* infection during the early lung larval stage.

IL-27 modulates the local presence of proinflammatory cytokines and chemokines.

To characterize the influence of IL-27 on the local milieu of inflammatory mediators, we employed a high-sensitive, multiplexed bead-based assay to quantify the concentrations of 26 cytokines and chemokines (Fig. 5, S3, S4). Il27ra$^{-/-}$ mice along with wild type (WT) control mice were inoculated with *N. brasiliensis* L3 and BALF was collected 2 days later. Significant differences were observed for 5 of 26 mediators. IL-6 concentrations were ~2-fold greater in Il27ra$^{-/-}$ mice (Fig. 5A). TNFα was also significantly increased in Il27ra$^{-/-}$ mice, although levels were near the lower detection

limit of the assay, possibly owing to the time point chosen (Fig. 5A). The macrophage and T cell-driving chemokine, MCP-3, was 2-fold higher in Il27ra$^{-/-}$ mice (Fig. 5A). In addition, we detected a trend towards lower concentrations for IL-23 ($p = 0.09$), a proinflammatory cytokine which is known to modulate T cell activity (Fig. 5A). Moreover, lower IL-10 concentrations and higher IL-17 amounts were detected (Fig. S3) in Il27ra$^{-/-}$ mice, which is consistent with the known requirement of IL-27 signaling to induce IL-10 from T cells and to suppress IL-17 responses in other disease models (32-34).

To further elaborate on the findings with Il27ra$^{-/-}$ mice, we measured inflammatory mediators in BALF of *N. brasiliensis* infected WT mice two days after a treatment regimen of rmIL-27 (100 ng i.p. on day 0 and day 1 p.i.) or mock injections. IL-6 was again observed to be present in abundant quantities, especially when considering the substantial dilution of alveolar lining fluid introduced by the lavage procedure (Fig. 5B). In contrast to the effect of IL-27 deficiency, IL-6 was suppressed by the addition of rmIL-27 (Fig. 5B). Likewise, mice that receive rmIL-27 were found to have lower TNFα and MCP-3 (Fig. 5B). Interestingly, no increase in IL-27 itself was detected in BALF 2 days after rmIL-27 injection (Fig. S4), suggesting clearance prior to that time point. In fact, we noticed a trend for suppressed (endogenous) IL-27 after injection, possibly attributable to a post excitation phenomenon.

Absence of IL-27 signaling decreases the expansion of γδ T cells in the alveolar space during primary N. brasiliensis infection

As T cells by far have the highest expression if IL-27RA (Fig. 2C-E), and all three T cell subsets evaluated express IL-27RA (albeit highest on TCRβ^{-}TCRγδ^{+} γδ T cells; Fig. 3), we next compared the percentage and number of all three T cells subsets in day 2 p.i. BAL between WT and Il27ra$^{-/-}$

315 mice. Compared to WT mice we observed a significant 1.4-fold reduction in the percentage of
316 $TCR\beta^{-}TCR\gamma\delta^{+}$ γδ T cells, a 1.3-fold reduction in percentage of $TCR\beta^{+}CD8^{+}$ CTLs and a slight
317 increase in percentage of $TCR\beta^{+}CD4^{+}$ Th cells (Fig. 6A, 6B) in $Il27ra^{-/-}$ mice. Moreover, BALs
318 from $Il27ra^{-/-}$ mice exhibited a 1.5-fold reduction in the absolute number of $TCR\beta^{-}TCR\gamma\delta^{+}$ γδ T
319 cells, while the counts of $TCR\beta^{+}CD4^{+}$ Th cells and $TCR\beta^{+}CD8^{+}$ CTLs were unchanged. Thus,
320 these findings support a role for IL-27 in enhancing the expansion of γδ T cells in the alveolar
321 space during primary *N. brasiliensis* infections of the lungs.
322

Discussion

In this report, we have identified a functional role for IL-27 signaling for protective immune defense against hookworm larvae, which migrate from the pulmonary vasculature into the airways. IL-27RA was expressed on all airway invading lymphocytes, albeit differentially based on cellular subset. IL-27RA was particularly abundant on γδ T cells compared to other innate and adaptive lymphocytes, suggesting this cell type as a prominent target for IL-27 mediated defense in the current setting. To this end, genetic deficiency of IL-27RA resulted in a greater parasite burden and more severe lung injury, whereas the opposite was true following IL-27 treatment. These findings were associated with differences in local proinflammatory cytokines and γδ T cell numbers in Il27ra$^{-/-}$ mice.

IL-27-dependent changes occurred within the first two days of infection, suggesting that its beneficial roles stem from alterations in innate immunity, especially given the time required for antigen-specific T cell responses. Yet, cytokine-induced T cells can modulate inflammation independently of their T cell receptor (35, 36), such that their accumulation in the airspaces may indeed contribute to the inflammatory milieu in some capacity.

Innate immunity to helminths is widely accepted to be limited to expulsion, a canonical type 2 response orchestrated by Th2 cells, ILC2s and γδ T2 IECs that, in the case of hookworm infections, is not initiated until the adult stage of the life cycle in the small intestine (13, 16). Innate immune mechanisms responsible for defense against helminth infections within the lungs has received much less attention, likely due to the gut being the conserved final destination for the majority of helminths. We demonstrate that there are mechanisms of innate resistance to hookworm infection in the lungs that are not necessarily associated with type 2 responses. As a key booster of pulmonary resistance to hookworms, we found that IL-27 is transiently induced for

346 expansion of γδ T cells in the alveolar space, where we anticipate their accumulation to directly
347 and/or indirectly eradicate larvae prior to their transition to the small intestine. Our results strongly
348 suggest that the role of IL-27 in the lung stage of hookworm infection is the opposite of the stage
349 in the gut, being anti-parasitic for the former and pro-parasitic for the latter (22).

350 The downregulation of IL-6 production by IL-27 (Fig. 5) may be a direct effect, since
351 lymphocytes can both produce and respond to IL-6 (37, 38). Alternatively, changes in IL-6 may
352 occur as an indirect consequence of IL-27RA-expressing NK cells and T cells dispatching signals
353 to control IL-6 synthesis in other non-lymphocytic cells. The precise role of IL-6 in lung injury
354 and pulmonary inflammation appears to be somewhat dependent on the disease model (39, 40).

355 The chemokine MCP-3 (CCL7) shares 71% sequence similarity with MCP-1 (CCL2) and
356 binds to the CCR2 receptor (41, 42). CCR2 is constitutively expressed not only on
357 monocytes/macrophages, but also on T cells, including IL-17 producing γδ T cells (43). However,
358 the higher concentrations of MCP-3 in Il27ra$^{-/-}$ mice during hookworm infection seem to contradict
359 the lower influx of γδ T cells in these mice (Fig. 5A vs. Fig. 6C). The increased MCP-3 may rather
360 represent an ineffective compensatory feedback loop to bring back up T cell numbers, when too
361 low. IL-27 itself is not a chemokine, but gp130-induced JAK/STAT1/STAT3 signaling may
362 regulate expression of chemokines, chemokine receptors and T cell migration (44, 45). Another
363 possibility is that elevated MCP-3 is secondary to the increase in pathogen burden resulting from
364 IL-27 deficiency, making the precise roles of MCP-3 speculative at present.

365 IL-27 is almost exclusively produced by macrophages and dendritic cells (20, 46). Here,
366 we have detected IL-27RA expression on all lung lymphocyte subpopulations during hookworm
367 infection, which is consistent with abundant evidence highlighting the responsiveness and
368 functional roles of IL-27 in T cells and B cells (20, 47). On the other hand, we did not observe IL-

27RA expression on mouse myeloid cells in lungs. In fact, the expression of IL-27RA on myeloid cells appears to occur in dependency of cell maturation and species (48-52). IL-27RA expression and IL-27 responsiveness exist for human neutrophils and human monocytes, whereas mouse macrophages only display minimal responsiveness (53, 54). We caution that none of the earlier reports have assessed IL-27RA expression in a cell-specific capacity (as accomplished by flow cytometry in the present study), but instead relied on RT-PCR or western blotting of cell lysates, making conclusive determination of cellular source somewhat speculative.

The regulatory role of IL-27 for the host immune defense against helminths does not appear to be limited to hookworms. Dual deficiency of IL-27RA and IL-10 rescues the great susceptibility of IL-10 single knockout mice for intestinal pathology and infection caused by the nematode *Trichuris muris* (55). *Strongyloides stercolaris*, the causative threadworm of Strongyloidiasis, infects more than 50 million people worldwide and infection results in a moderate but significant increase of IL-27 in human plasma, which decreases after anthelmintic treatment (56).

In human whole blood cultures of infected individuals re-stimulated with recombinant *S. stercolaris* NIE antigen, the neutralization of IL-27 using antibodies increased the frequencies of all $CD4^+$ T helper cell subsets (T_{h1}-T_{h22}), $CD8^+$ T cells and modulated cytokine levels (57). *Ascaris lubricoides* antigen induced IL-27 release from PBMCs in adults and the elderly as compared to neonates and children of an endemic cohort from Sub-Saharan Africa, with a 30% prevalence of hook worm infections and multiple parasite infections (58). Altogether, these observations suggest an important influence of IL-27 on host outcome in a variety of settings of helminthic infections.

The mechanisms of innate immune recognition for helminths remain unclear. No dedicated class of pattern recognition receptors has been identified so far. Helminth-derived chitin, proteoglycans, lipids and excretory-secretory products may be recognized by TLRs and C-type

lectins (59, 60). In addition, danger associated molecular patterns (DAMPs) when released during helminth-induced tissue injury could act as endogenous ligands for TLRs (and other receptors), thereby inducing MYD88/TRIF-dependent IL-27 production (46, 61, 62). Furthermore, γδ T cells can be activated by DAMPs from mitochondria (63).

While we describe in this report that recombinant IL-27 reinforced the anthelmintic host defense in the lungs, the feasibility of proposing its administration as an effective therapy is highly speculative. First, the efficacy observed in our studies was less than 50% for reduction of the lung larvae burden in IL-27-treated mice, although this could be improved by further dose optimization. Secondly, the skin penetration of hookworm larvae in humans usually is unnoticed, such that any window of therapeutic efficacy may be too difficult to rely on. Thirdly, another report showed that a non-viral minicircle DNA vector injected intra-venously for recombinant expression of IL-27 resulted in higher numbers of adult *N. brasiliensis* in the intestinal tract (22). This implies that the role of IL-27 could be either protective or detrimental depending on the stage of the hookworm infection cycle and host tissue environment. It appears that more sophisticated manipulations would be needed to specifically enhance IL-27-dependent protective immunity in the lung. IL-27 may be an interesting factor to explore for developing adjuvants for vaccines that target the early lung stage of human hookworms (11). Vaccine adjuvants would need to be tailored to locally induce IL-27 (27-29), or to up-regulate IL-27RA expression and IL-27 responsiveness of lung resident lymphocyte subpopulations (64).

In conclusion, the presented work expands on the emerging role of IL-27 as a critical factor of host defense and immune regulation against hookworm infections. The pulmonary stage of the parasitic infection cycle remains an understudied area and we highlight the importance to better understand the lung lymphocyte-specific host response. In the future, more research will be needed

to fully uncover the intricate molecular mechanisms of host-helminth interactions as a basis for developing innovative treatment approaches against this neglected tropical disease.

Acknowledgments

We thank Dr. Joseph Urban Jr. (USDA, Beltsville, MD) for kindly providing the murine hookworm *N. brasiliensis*. This work was supported by the National Institutes of Health (1R01HL141513, 1R01HL139641 to M.B.), the Federal Ministry of Education and Research (01EO1503 to M.B. and C.R.), the Deutsche Forschungsgemeinschaft (BO3482/3-3, BO3482/4-1 to M.B. and RE-3450/5-2 to C.R.), a Marie Curie Career Integration Grant of the European Union (Project 334486 to M.B.), a Clinical Research Fellowship of the European Hematology Association (to M.B.) and a project grant from the Boehringer Ingelheim Foundation (Consortium Grant "Novel and neglected cardiovascular risk factors" to C.R.). C.R. was awarded a fellowship from the Gutenberg Research College. The authors are responsible for the contents of this publication.

Author Contributions

J.B.N. and A.S. designed and performed experiments and analyzed data. J.P. and C.R. contributed to experimental designs and provided helpful comments. M.B. conceived and supervised the study, designed experiments, interpreted data and provided funding. J.B.N. and M.B. wrote the manuscript, which was further edited by A.S., L.J.Q. and C.R.

Correspondence and requests for materials

Requests for materials and correspondence should be addressed to M.B.

Disclosures

The authors have no financial conflicts of interest.

References

1. Loukas, A., P. J. Hotez, D. Diemert, M. Yazdanbakhsh, J. S. McCarthy, R. Correa-Oliveira, J. Croese, and J. M. Bethony. 2016. Hookworm infection. *Nat Rev Dis Primers* 2: 16088.
2. Pullan, R. L., J. L. Smith, R. Jasrasaria, and S. J. Brooker. 2014. Global numbers of infection and disease burden of soil transmitted helminth infections in 2010. *Parasit Vectors* 7: 37.
3. Herricks, J. R., P. J. Hotez, V. Wanga, L. E. Coffeng, J. A. Haagsma, M. G. Basanez, G. Buckle, C. M. Budke, H. Carabin, E. M. Fevre, T. Furst, Y. A. Halasa, C. H. King, M. E. Murdoch, K. D. Ramaiah, D. S. Shepard, W. A. Stolk, E. A. Undurraga, J. D. Stanaway, M. Naghavi, and C. J. L. Murray. 2017. The global burden of disease study 2013: What does it mean for the NTDs? *PLoS Negl Trop Dis* 11: e0005424.
4. Brooker, S., P. J. Hotez, and D. A. Bundy. 2008. Hookworm-related anaemia among pregnant women: a systematic review. *PLoS Negl Trop Dis* 2: e291.
5. Smith, J. L., and S. Brooker. 2010. Impact of hookworm infection and deworming on anaemia in non-pregnant populations: a systematic review. *Trop Med Int Health* 15: 776-795.
6. Hotez, P. J., S. Brooker, J. M. Bethony, M. E. Bottazzi, A. Loukas, and S. Xiao. 2004. Hookworm infection. *N Engl J Med* 351: 799-807.
7. Kassebaum, N. J., and G. B. D. A. Collaborators. 2016. The Global Burden of Anemia. *Hematol Oncol Clin North Am* 30: 247-308.
8. Hotez, P. J., D. A. P. Bundy, K. Beegle, S. Brooker, L. Drake, N. de Silva, A. Montresor, D. Engels, M. Jukes, L. Chitsulo, J. Chow, R. Laxminarayan, C. Michaud, J. Bethony, R. Correa-Oliveira, X. Shuhua, A. Fenwick, and L. Savioli. 2006. Helminth Infections: Soil-transmitted Helminth Infections and Schistosomiasis. In *Disease Control Priorities in Developing Countries*. nd, D. T. Jamison, J. G. Breman, A. R. Measham, G. Alleyne, M. Claeson, D. B. Evans, P. Jha, A. Mills, and P. Musgrove, eds, Washington (DC).
9. Anderson, R., J. Truscott, and T. D. Hollingsworth. 2014. The coverage and frequency of mass drug administration required to eliminate persistent transmission of soil-transmitted helminths. *Philos Trans R Soc Lond B Biol Sci* 369: 20130435.
10. Bethony, J., S. Brooker, M. Albonico, S. M. Geiger, A. Loukas, D. Diemert, and P. J. Hotez. 2006. Soil-transmitted helminth infections: ascariasis, trichuriasis, and hookworm. *Lancet* 367: 1521-1532.
11. Noon, J. B., and R. V. Aroian. 2017. Recombinant subunit vaccines for soil-transmitted helminths. *Parasitology* 144: 1845-1870.
12. Camberis, M., G. Le Gros, and J. Urban, Jr. 2003. Animal model of Nippostrongylus brasiliensis and Heligmosomoides polygyrus. *Curr Protoc Immunol* Chapter 19: Unit 19 12.
13. Nair, M. G., and D. R. Herbert. 2016. Immune polarization by hookworms: taking cues from T helper type 2, type 2 innate lymphoid cells and alternatively activated macrophages. *Immunology* 148: 115-124.
14. Sutherland, T. E., N. Logan, D. Ruckerl, A. A. Humbles, S. M. Allan, V. Papayannopoulos, B. Stockinger, R. M. Maizels, and J. E. Allen. 2014. Chitinase-like proteins promote IL-17-mediated neutrophilia in a tradeoff between nematode killing and host damage. *Nat Immunol* 15: 1116-1125.

15. Cardoso, V., J. Chesne, H. Ribeiro, B. Garcia-Cassani, T. Carvalho, T. Bouchery, K. Shah, N. L. Barbosa-Morais, N. Harris, and H. Veiga-Fernandes. 2017. Neuronal regulation of type 2 innate lymphoid cells via neuromedin U. *Nature* 549: 277-281.
16. Inagaki-Ohara, K., Y. Sakamoto, T. Dohi, and A. L. Smith. 2011. gammadelta T cells play a protective role during infection with Nippostrongylus brasiliensis by promoting goblet cell function in the small intestine. *Immunology* 134: 448-458.
17. Pflanz, S., J. C. Timans, J. Cheung, R. Rosales, H. Kanzler, J. Gilbert, L. Hibbert, T. Churakova, M. Travis, E. Vaisberg, W. M. Blumenschein, J. D. Mattson, J. L. Wagner, W. To, S. Zurawski, T. K. McClanahan, D. M. Gorman, J. F. Bazan, R. de Waal Malefyt, D. Rennick, and R. A. Kastelein. 2002. IL-27, a heterodimeric cytokine composed of EBI3 and p28 protein, induces proliferation of naive CD4(+) T cells. *Immunity* 16: 779-790.
18. Collison, L. W., C. J. Workman, T. T. Kuo, K. Boyd, Y. Wang, K. M. Vignali, R. Cross, D. Sehy, R. S. Blumberg, and D. A. Vignali. 2007. The inhibitory cytokine IL-35 contributes to regulatory T-cell function. *Nature* 450: 566-569.
19. Hamano, S., K. Himeno, Y. Miyazaki, K. Ishii, A. Yamanaka, A. Takeda, M. Zhang, H. Hisaeda, T. W. Mak, A. Yoshimura, and H. Yoshida. 2003. WSX-1 is required for resistance to Trypanosoma cruzi infection by regulation of proinflammatory cytokine production. *Immunity* 19: 657-667.
20. Bosmann, M., and P. A. Ward. 2013. Modulation of inflammation by interleukin-27. *J Leukoc Biol* 94: 1159-1165.
21. Hunter, C. A., and R. Kastelein. 2012. Interleukin-27: balancing protective and pathological immunity. *Immunity* 37: 960-969.
22. McHedlidze, T., M. Kindermann, A. T. Neves, D. Voehringer, M. F. Neurath, and S. Wirtz. 2016. IL-27 suppresses type 2 immune responses in vivo via direct effects on group 2 innate lymphoid cells. *Mucosal Immunol* 9: 1384-1394.
23. Artis, D., A. Villarino, M. Silverman, W. He, E. M. Thornton, S. Mu, S. Summer, T. M. Covey, E. Huang, H. Yoshida, G. Koretzky, M. Goldschmidt, G. D. Wu, F. de Sauvage, H. R. Miller, C. J. Saris, P. Scott, and C. A. Hunter. 2004. The IL-27 receptor (WSX-1) is an inhibitor of innate and adaptive elements of type 2 immunity. *J Immunol* 173: 5626-5634.
24. Filbey, K., T. Bouchery, and G. Le Gros. 2018. The role of ILC2 in hookworm infection. *Parasite Immunol* 40.
25. Fallon, P. G., S. J. Ballantyne, N. E. Mangan, J. L. Barlow, A. Dasvarma, D. R. Hewett, A. McIlgorm, H. E. Jolin, and A. N. McKenzie. 2006. Identification of an interleukin (IL)-25-dependent cell population that provides IL-4, IL-5, and IL-13 at the onset of helminth expulsion. *J Exp Med* 203: 1105-1116.
26. Moro, K., H. Kabata, M. Tanabe, S. Koga, N. Takeno, M. Mochizuki, K. Fukunaga, K. Asano, T. Betsuyaku, and S. Koyasu. 2016. Interferon and IL-27 antagonize the function of group 2 innate lymphoid cells and type 2 innate immune responses. *Nat Immunol* 17: 76-86.
27. Pennock, N. D., L. Gapin, and R. M. Kedl. 2014. IL-27 is required for shaping the magnitude, affinity distribution, and memory of T cells responding to subunit immunization. *Proc Natl Acad Sci U S A* 111: 16472-16477.

28. Kilgore, A. M., N. D. Pennock, and R. M. Kedl. 2020. cDC1 IL-27p28 Production Predicts Vaccine-Elicited CD8(+) T Cell Memory and Protective Immunity. *J Immunol* 204: 510-517.
29. Coffman, R. L., A. Sher, and R. A. Seder. 2010. Vaccine adjuvants: putting innate immunity to work. *Immunity* 33: 492-503.
30. Oshiro, I., T. Takenaka, and J. Maeda. 1982. New method for hemoglobin determination by using sodium lauryl sulfate (SLS). *Clin Biochem* 15: 83-88.
31. Bosmann, M., N. F. Russkamp, V. R. Patel, F. S. Zetoune, J. V. Sarma, and P. A. Ward. 2011. The outcome of polymicrobial sepsis is independent of T and B cells. *Shock* 36: 396-401.
32. Batten, M., J. Li, S. Yi, N. M. Kljavin, D. M. Danilenko, S. Lucas, J. Lee, F. J. de Sauvage, and N. Ghilardi. 2006. Interleukin 27 limits autoimmune encephalomyelitis by suppressing the development of interleukin 17-producing T cells. *Nature Immunology* 7: 929-936.
33. Stumhofer, J. S., A. Laurence, E. H. Wilson, E. Huang, C. M. Tato, L. M. Johnson, A. V. Villarino, Q. Huang, A. Yoshimura, D. Sehy, C. J. Saris, J. J. O'Shea, L. Hennighausen, M. Ernst, and C. A. Hunter. 2006. Interleukin 27 negatively regulates the development of interleukin 17-producing T helper cells during chronic inflammation of the central nervous system. *Nat Immunol* 7: 937-945.
34. Stumhofer, J. S., J. S. Silver, A. Laurence, P. M. Porrett, T. H. Harris, L. A. Turka, M. Ernst, C. J. Saris, J. J. O'Shea, and C. A. Hunter. 2007. Interleukins 27 and 6 induce STAT3-mediated T cell production of interleukin 10. *Nat Immunol* 8: 1363-1371.
35. Schmidt-Wolf, I. G., R. S. Negrin, H. P. Kiem, K. G. Blume, and I. L. Weissman. 1991. Use of a SCID mouse/human lymphoma model to evaluate cytokine-induced killer cells with potent antitumor cell activity. *J Exp Med* 174: 139-149.
36. Meresse, B., Z. Chen, C. Ciszewski, M. Tretiakova, G. Bhagat, T. N. Krausz, D. H. Raulet, L. L. Lanier, V. Groh, T. Spies, E. C. Ebert, P. H. Green, and B. Jabri. 2004. Coordinated induction by IL15 of a TCR-independent NKG2D signaling pathway converts CTL into lymphokine-activated killer cells in celiac disease. *Immunity* 21: 357-366.
37. Avanzi, G. C., A. Cessano, M. F. Brizzi, S. C. Clark, L. Pegoraro, and L. Matera. 1989. Biological and molecular evidence for the production of IL-6 by human natural killer cells in culture. *Life Sci* 45: 2621-2626.
38. Kuhn, K. A., N. A. Manieri, T. C. Liu, and T. S. Stappenbeck. 2014. IL-6 stimulates intestinal epithelial proliferation and repair after injury. *PLoS One* 9: e114195.
39. Saito, F., S. Tasaka, K. Inoue, K. Miyamoto, Y. Nakano, Y. Ogawa, W. Yamada, Y. Shiraishi, N. Hasegawa, S. Fujishima, H. Takano, and A. Ishizaka. 2008. Role of interleukin-6 in bleomycin-induced lung inflammatory changes in mice. *Am J Respir Cell Mol Biol* 38: 566-571.
40. Bhargava, R., W. Janssen, C. Altmann, A. Andres-Hernando, K. Okamura, R. W. Vandivier, N. Ahuja, and S. Faubel. 2013. Intratracheal IL-6 protects against lung inflammation in direct, but not indirect, causes of acute lung injury in mice. *PLoS One* 8: e61405.
41. Sozzani, S., D. Zhou, M. Locati, M. Rieppi, P. Proost, M. Magazin, N. Vita, J. van Damme, and A. Mantovani. 1994. Receptors and transduction pathways for monocyte

chemotactic protein-2 and monocyte chemotactic protein-3. Similarities and differences with MCP-1. *J Immunol* 152: 3615-3622.

42. Franci, C., L. M. Wong, J. Van Damme, P. Proost, and I. F. Charo. 1995. Monocyte chemoattractant protein-3, but not monocyte chemoattractant protein-2, is a functional ligand of the human monocyte chemoattractant protein-1 receptor. *J Immunol* 154: 6511-6517.

43. McKenzie, D. R., E. E. Kara, C. R. Bastow, T. S. Tyllis, K. A. Fenix, C. E. Gregor, J. J. Wilson, R. Babb, J. C. Paton, A. Kallies, S. L. Nutt, A. Brustle, M. Mack, I. Comerford, and S. R. McColl. 2017. IL-17-producing gammadelta T cells switch migratory patterns between resting and activated states. *Nat Commun* 8: 15632.

44. McLoughlin, R. M., B. J. Jenkins, D. Grail, A. S. Williams, C. A. Fielding, C. R. Parker, M. Ernst, N. Topley, and S. A. Jones. 2005. IL-6 trans-signaling via STAT3 directs T cell infiltration in acute inflammation. *Proc Natl Acad Sci U S A* 102: 9589-9594.

45. Barbi, J., S. Oghumu, C. M. Lezama-Davila, and A. R. Satoskar. 2007. IFN-gamma and STAT1 are required for efficient induction of CXC chemokine receptor 3 (CXCR3) on CD4+ but not CD8+ T cells. *Blood* 110: 2215-2216.

46. Bosmann, M., N. F. Russkamp, B. Strobl, J. Roewe, L. Balouzian, F. Pache, M. P. Radsak, N. van Rooijen, F. S. Zetoune, J. V. Sarma, G. Nunez, M. Muller, P. J. Murray, and P. A. Ward. 2014. Interruption of macrophage-derived IL-27(p28) production by IL-10 during sepsis requires STAT3 but not SOCS3. *J Immunol* 193: 5668-5677.

47. Vijayan, D., N. Mohd Redzwan, D. T. Avery, R. C. Wirasinha, R. Brink, G. Walters, S. Adelstein, M. Kobayashi, P. Gray, M. Elliott, M. Wong, C. King, C. G. Vinuesa, N. Ghilardi, C. S. Ma, S. G. Tangye, and M. Batten. 2016. IL-27 Directly Enhances Germinal Center B Cell Activity and Potentiates Lupus in Sanroque Mice. *J Immunol* 197: 3008-3017.

48. Pflanz, S., L. Hibbert, J. Mattson, R. Rosales, E. Vaisberg, J. F. Bazan, J. H. Phillips, T. K. McClanahan, R. de Waal Malefyt, and R. A. Kastelein. 2004. WSX-1 and glycoprotein 130 constitute a signal-transducing receptor for IL-27. *J Immunol* 172: 2225-2231.

49. Kalliolias, G. D., and L. B. Ivashkiv. 2008. IL-27 activates human monocytes via STAT1 and suppresses IL-10 production but the inflammatory functions of IL-27 are abrogated by TLRs and p38. *J Immunol* 180: 6325-6333.

50. Holscher, C., A. Holscher, D. Ruckerl, T. Yoshimoto, H. Yoshida, T. Mak, C. Saris, and S. Ehlers. 2005. The IL-27 receptor chain WSX-1 differentially regulates antibacterial immunity and survival during experimental tuberculosis. *J Immunol* 174: 3534-3544.

51. Zhao, X., S. M. Ting, C. H. Liu, G. Sun, M. Kruzel, M. Roy-O'Reilly, and J. Aronowski. 2017. Neutrophil polarization by IL-27 as a therapeutic target for intracerebral hemorrhage. *Nat Commun* 8: 602.

52. Seita, J., M. Asakawa, J. Ooehara, S. Takayanagi, Y. Morita, N. Watanabe, K. Fujita, M. Kudo, J. Mizuguchi, H. Ema, H. Nakauchi, and T. Yoshimoto. 2008. Interleukin-27 directly induces differentiation in hematopoietic stem cells. *Blood* 111: 1903-1912.

53. Li, J. P., H. Wu, W. Xing, S. G. Yang, S. H. Lu, W. T. Du, J. X. Yu, F. Chen, L. Zhang, and Z. C. Han. 2010. Interleukin-27 as a negative regulator of human neutrophil function. *Scand J Immunol* 72: 284-292.

54. Ruckerl, D., M. Hessmann, T. Yoshimoto, S. Ehlers, and C. Holscher. 2006. Alternatively activated macrophages express the IL-27 receptor alpha chain WSX-1. *Immunobiology* 211: 427-436.
55. Villarino, A. V., D. Artis, J. S. Bezbradica, O. Miller, C. J. Saris, S. Joyce, and C. A. Hunter. 2008. IL-27R deficiency delays the onset of colitis and protects from helminth-induced pathology in a model of chronic IBD. *Int Immunol* 20: 739-752.
56. Anuradha, R., S. Munisankar, Y. Bhootra, J. Jagannathan, C. Dolla, P. Kumaran, K. Shen, T. B. Nutman, and S. Babu. 2016. Systemic Cytokine Profiles in Strongyloides stercoralis Infection and Alterations following Treatment. *Infect Immun* 84: 425-431.
57. Anuradha, R., S. Munisankar, Y. Bhootra, C. Dolla, P. Kumaran, T. B. Nutman, and S. Babu. 2017. Modulation of CD4(+) and CD8(+) T Cell Function and Cytokine Responses in Strongyloides stercoralis Infection by Interleukin-27 (IL-27) and IL-37. *Infect Immun* 85.
58. Hegewald, J., R. G. Gantin, C. J. Lechner, X. Huang, A. Agosssou, Y. F. Agbeko, P. T. Soboslay, and C. Kohler. 2015. Cellular cytokine and chemokine responses to parasite antigens and fungus and mite allergens in children co-infected with helminthes and protozoa parasites. *J Inflamm (Lond)* 12: 5.
59. Perrigoue, J. G., F. A. Marshall, and D. Artis. 2008. On the hunt for helminths: innate immune cells in the recognition and response to helminth parasites. *Cell Microbiol* 10: 1757-1764.
60. McGuinness, D. H., P. K. Dehal, and R. J. Pleass. 2003. Pattern recognition molecules and innate immunity to parasites. *Trends Parasitol* 19: 312-319.
61. Bosmann, M., M. D. Haggadone, M. R. Hemmila, F. S. Zetoune, J. V. Sarma, and P. A. Ward. 2012. Complement activation product C5a is a selective suppressor of TLR4-induced, but not TLR3-induced, production of IL-27(p28) from macrophages. *J Immunol* 188: 5086-5093.
62. Bosmann, M., B. Strobl, N. Kichler, D. Rigler, J. J. Grailer, F. Pache, P. J. Murray, M. Muller, and P. A. Ward. 2014. Tyrosine kinase 2 promotes sepsis-associated lethality by facilitating production of interleukin-27. *J Leukoc Biol* 96: 123-131.
63. Schwacha, M. G., M. Rani, S. E. Nicholson, A. M. Lewis, T. L. Holloway, S. Sordo, and A. P. Cap. 2016. Dermal gammadelta T-Cells Can Be Activated by Mitochondrial Damage-Associated Molecular Patterns. *PLoS One* 11: e0158993.
64. Szabo, P. A., M. Miron, and D. L. Farber. 2019. Location, location, location: Tissue resident memory T cells in mice and humans. *Sci Immunol* 4.

Figure Legends

FIGURE 1. IL-27(p28) is transiently present in the lung alveolar space at day 1 post-inoculation with *N. brasiliensis* larvae.

Wild type mice (C57BL/6J) were inoculated s.c. with L3 larvae (n=500/mouse) of *N. brasiliensis*. IL-27(p28) was quantified in broncho-alveolar lavage fluids (BALF) by ELISA at the indicated time points (days 0, 1, 2 and 9). Comparisons of mean ± SEM and each circle represents an individual animal. PBS: mock inoculated/uninfected/day 0 post-inoculation. * $P<0.05$, **** $P<0.0001$, ns: not significant.

FIGURE 2. *N. brasiliensis* infection promotes the appearance of IL-27RA expressing lymphocytes in the lungs. C57BL/6J wild type mice were infected s.c. with L3 larvae (n=500/mouse) or received a mock PBS injection as controls. The inflammatory cells were collected by BAL at indicated time points and analyzed by flow cytometry.

(**A**) Plots of CD19 versus CD3 pre-gated on $CD45^+Ly6G^-$ single cell lymphocytes (left panel) and NK1.1 versus CD3 gated on $CD19^-CD3^-$ innate lymphocytes (right panel) at 2 days after infection. Percentages are indicated next to each gate. (**B**) Absolute numbers of lymphocyte populations in BAL of $CD19^-CD3^+$ T cells, $CD19^+CD3^-$ B cells and $CD19^-CD3^-NK1.1^+$ NK cells on day 0 (PBS-inoculated/uninfected), day 1 and day 2 post-inoculation (n=3 mice/group). (**C**) Representative histograms of IL-27RA expression on $CD19^-CD3^+$ T cells. (left panel), $CD19^-CD3^-NK1.1^+$ NK cells (middle panel) and $CD19^+CD3^-$ B cells (right panel) on day 2 p.i. The dotted black line indicates isotype-FMO control. The percentages of $IL\text{-}27RA^-$ and $IL\text{-}27RA^+$ cells are indicated in the upper left and right corners, respectively. (**D**) Frequencies (%) of $IL\text{-}27RA^+CD19^-CD3^+$ T

cells, $CD19^{-}CD3^{-}NK1.1^{+}$ NK cells and $CD19^{+}CD3^{-}$ B cells in BAL on day 1 (n=2 mice/group) and day 2 (n=3 mice/group) post-inoculation. (**E**) IL-27RA presence expressed as geometric mean fluorescence intensities (gMFI) on $CD19^{-}CD3^{+}$ T cells, $CD19^{-}CD3^{-}NK1.1^{+}$ NK cells and $CD19^{+}CD3^{-}$ B cells (all left panel) from the same experiments described in frame D. A representative histogram of IL-27RA expression on $CD19^{-}CD3^{+}$ T cells is shown in the right panel with the dotted and solid red lines indicating days 1 and 2 p.i., respectively. The dotted black line indicates isotype-FMO control (Ctrl). Data (B, D, E) are shown as mean ± SEM and were analyzed by two-tailed t-test (B) comparing day 0 vs. day 1 and day 0 vs. day 2 for each cell type, or two-way ANOVA (D, E), * $P<0.05$, ** $P<0.01$, *** $P<0.001$, **** $P<0.0001$, ns: not significant.

FIGURE 3. IL-27RA expression is highest on γδ T cells among broncho-alveolar lymphocytes during *N. brasiliensis* infection.

(**A**) Flow cytometry plots of TCRβ chain versus TCRγδ pre-gated on $CD3^{+}$ single cell lymphocytes (left panel) and CD4 versus CD8a on αβ T cells (right panel) in BAL after 2 days of infection with L3 larvae of *N. brasiliensis* (n=500 per C57BL/6/J mouse s.c.). The frequencies (%) of cells are indicated next to each gate. (**B**) Absolute numbers in BAL of $CD4^{+}CD8^{-}$ T helper (Th) cells, $CD4^{-}CD8^{+}$ cytotoxic T lymphocytes (CTLs) and $TCR\beta^{-}TCR\gamma\delta^{+}$ γδ T cells on day 0 (PBS-inoculated/uninfected), day 1 (n=2 mice/group) and day 2 post-inoculation (n=6 mice/group). (**C**) Representative histograms of IL-27RA expression on $TCR\beta^{-}TCR\gamma\delta^{+}$ γδ T cells (left panel), $CD4^{-}CD8^{+}$ CTLs (middle panel) and $CD4^{+}CD8^{-}$ Th cells (right panel). The dotted line indicates IL-27RA staining in $Il27ra^{-/-}$ mice as negative control. The percentages of $IL\text{-}27RA^{-}$ and $IL\text{-}27RA^{+}$ cells are indicated in the upper left and right corners, respectively. (**D**) Relative numbers of IL-27RA-positive $TCR\beta^{-}TCR\gamma\delta^{+}$ γδ T cells, $CD4^{-}CD8^{+}$ CTLs and $CD4^{+}CD8^{-}$ Th cells in BAL on day

2 p.i. (n=6 mice/group). (**E**) IL-27RA abundance (gMFI) on TCRβ^{-}TCRγδ^{+} γδ T cells, CD4^{-}CD8^{+} CTLs and CD4^{+}CD8^{-} Th cells in BAL on day 2 p.i. (n=6 mice/group). Data (B, D, E) are shown as mean ± SEM and were analyzed by two-tailed t-test (B) comparing day 0 vs. day 1 and day 0 vs. day 2 for each cell type, or one-way ANOVA (D, E), * P<0.05, ** P<0.01, *** P<0.001, **** P<0.0001, ns: not significant.

FIGURE 4. IL-27 enhances innate resistance to primary *N. brasiliensis* infection in the lungs.

(**A-C**) *In vivo* comparison of susceptibility of Il27ra$^{-/-}$ mice and wild type (WT; C57BL/6NJ) mice to primary *N. brasiliensis* infection (L3 n=500/mouse) in the lungs at 2 days after infection. (**A**) Alveolar parasite burden, (**B**) alveolar hemorrhage, and (**C**) alveolar total protein in BALF. (**D-F**) *In vivo* comparison of susceptibility of WT mice (C57BL/6J) administered with rmIL-27 (100 ng/mouse i.p., once daily on days 0-1) or mock control (0.1% BSA in PBS) during *N. brasiliensis* infection and analyzed after 2 days p.i. (**D**) Comparison of alveolar parasite burden, (**E**) alveolar hemorrhage, and (**F**) alveolar total protein in BALF. Data (A-F) are shown as mean ± SEM and each circle indicates an individual mouse, * P<0.05, ** P<0.01, ns: not significant.

FIGURE 5. IL-27 regulates inflammatory mediators during primary pulmonary *N. brasiliensis* infection.

(**A**) *In vivo* comparison of selected cytokines and chemokines of Il27ra$^{-/-}$ mice and wild type control (C57BL/6NJ) mice to primary *N. brasiliensis* infection (L3 n=500/mouse) in the lungs (BALF) at 2 days after infection. (**B**) C57BL/6J mice administered with rmIL-27 (100 ng/mouse i.p., once daily on day 0 and day 1) or mock control (0.1% BSA in PBS) during *N. brasiliensis* infection and analyzed for the presence of inflammatory mediators after 2 days p.i in BALF. All

data were obtained by multiplexed bead-based assay (Luminex-200). Graphs (A-B) are presented as mean ± SEM, were analyzed by two-tailed t-test and each circle indicates an individual mouse, * $P<0.05$, ** $P<0.01$.

FIGURE 6. Il27ra$^{-/-}$ mice have decreased presence of γδ T cells in the alveolar space during *N. brasiliensis* infection.

(**A**) Representative flow cytometry plots of TCRβ^{-}TCRγδ^{+} γδ T cells (top panel), and CD4^{+}CD8^{-} Th cells and CD4^{-}CD8^{+} CTLs (bottom panel), gated as in Fig. 3A, for WT (left panel) and Il27ra$^{-/-}$ mice (right panel) in BAL on day 2 p.i. Percentages are indicated next to each gate. (**B**, **C**) Comparisons of frequencies (B) and absolute numbers (C) of CD4^{+}CD8^{-} Th cells, CD4^{-}CD8^{+} CTLs and TCRβ^{-}TCRγδ^{+} γδ T cells in BAL of WT mice (n=5 mice/group; one mouse was removed due to extremely low infection, as determined by negligible hemorrhage) and Il27ra$^{-/-}$ mice on day 2 p.i. (n=6 mice/group). Data (B, C) are shown as mean ± SEM, were analyzed by two-tailed t-test (WT vs. Il27ra$^{-/-}$) and each symbol represents the value of an individual mouse, * $P<0.05$, ns: not significant.

FIGURE S1. IL-27RA is not expressed on alveolar macrophages, neutrophils or eosinophils from the alveolar space during *N. brasiliensis* infection.

(**A**) Flow cytometry plots including gating strategy of CD45 versus Ly6G pre-gated on single myeloid cells (left) and CD11c versus Siglec-F on Ly6G^{-} myeloid cells (right). Percentages are indicated next to each gate. (**B**) Numbers of Ly6G^{+} neutrophils, Ly6G^{-}CD11c^{+}Siglec-F^{+} alveolar macrophages and Ly6G^{-}CD11c^{-}Siglec-F^{+} eosinophils on day 0 (PBS-inoculated/uninfected), day 1 and day 2 post-inoculation (n=3 mice/group) in BAL; day 0 vs. day 1 and day 0 vs. day 2 using two-tailed t-test, data shows mean ± SEM. (**C**) Histograms of IL-27RA expression on Ly6G^{-}

749 $CD11c^{+}Siglec\text{-}F^{+}$ alveolar macrophages (left), $Ly6G^{+}$ neutrophils (middle) and $Ly6G^{-}CD11c^{-}$
750 $Siglec\text{-}F^{+}$ eosinophils (right) on day 2 p.i. The dotted line indicates isotype-FMO control. The
751 percentages of $IL\text{-}27RA^{-}$ and $IL\text{-}27RA^{+}$ cells are indicated in the upper left and right corners,
752 respectively.
753
754 **FIGURE S2.** Parasite burdens are similar between wild type mice compared to $Il27ra^{-/-}$ mice in
755 the lung tissues during *N. brasiliensis* infection.
756 Wild type mice (C57BL/6NJ) and $Il27ra^{-/-}$ mice were inoculated s.c. with L3 larvae
757 (n=500/mouse). Parasite numbers were counted in whole lung tissues after removal of intra-airway
758 parasites by multiple BAL on day 2 of infection. Lungs were minced from the same experiments
759 as shown in Fig. 4A. Comparison of mean ± SEM analyzed by two-tailed t-test and each circle
760 indicates the value of an individual mouse, ns: not significant.
761
762 **FIGURE S3.** Cytokines and chemokines in brochoalveolar lavage fluids of $Il27ra^{-/-}$ mice.
763 *In vivo* comparison of different cytokines and chemokines of $Il27ra^{-/-}$ mice and wild type (WT;
764 C57BL/6NJ) mice during primary *N. brasiliensis* infection (L3 n=500/mouse) in BALF after 2
765 days, bead-based multiplex assay. Data are shown as mean ± SEM and each circle represents an
766 individual mouse, two-tailed t-test, * $P<0.05$, ** $P<0.01$.
767
768 **FIGURE S4.** Cytokines and chemokines in brochoalveolar lavage fluids after treatment with
769 recombinant mouse IL-27.
770 *In vivo* comparison of mediators in BALF from WT mice (C57BL/6J) administered with rmIL-27
771 (100 ng/mouse i.p.) or mock control (0.1% BSA in PBS) on day 0 and day 1 of *N. brasiliensis*

772 infection and analyzed after 2 days p.i. Data are shown as mean ± SEM and each circle indicates

773 an individual mouse, two-tailed t-test, * $P<0.05$.

Figure 1

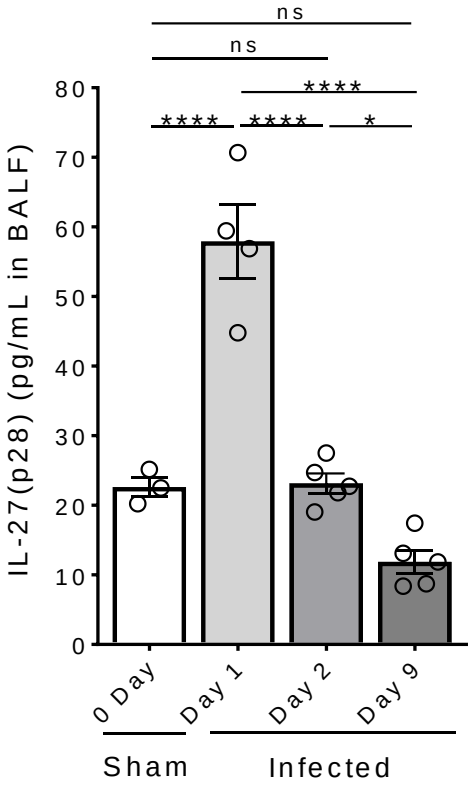
ns
ns
****
****
****
*
IL-27(p28) (pg/mL in BALF)
80
70
60
50
40
30
20
10
0
0 Day
Day 1
Day 2
Day 9
Sham
Infected

Figure 2

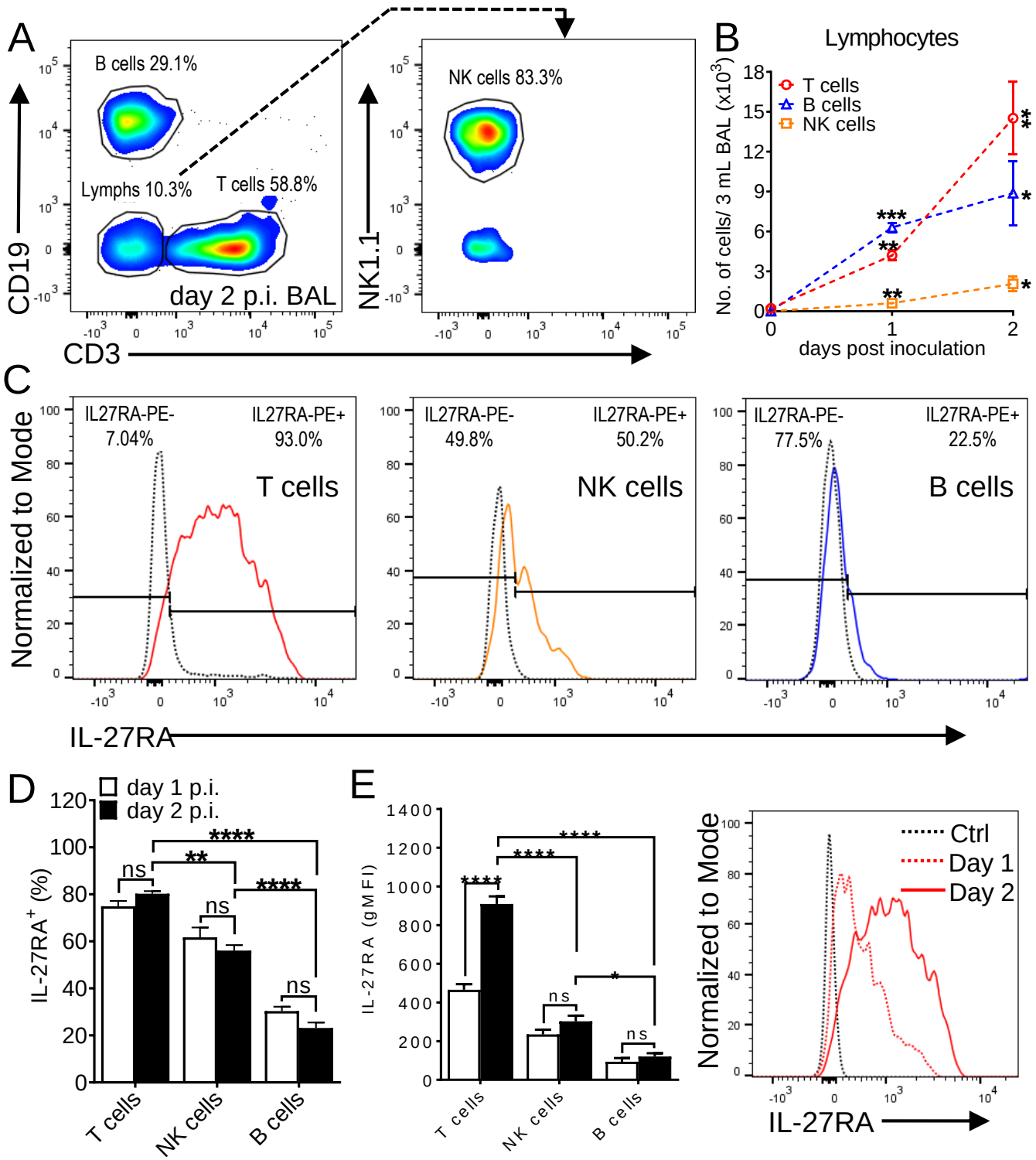
A
B cells 29.1%
Lymphs 10.3%
T cells 58.8%
day 2 p.i. BAL
CD19
CD3
NK cells 83.3%
NK1.1
B
Lymphocytes
T cells
B cells
NK cells
No. of cells/ 3 mL BAL (x10^3)
days post inoculation
C
Normalized to Mode
IL27RA-PE- 7.04%
IL27RA-PE+ 93.0%
T cells
IL27RA-PE- 49.8%
IL27RA-PE+ 50.2%
NK cells
IL27RA-PE- 77.5%
IL27RA-PE+ 22.5%
B cells
IL-27RA
D
day 1 p.i.
day 2 p.i.
IL-27RA+ (%)
ns
**
****
T cells
NK cells
B cells
E
IL-27RA (gMFI)
*
Ctrl
Day 1
Day 2
Normalized to Mode
IL-27RA

Figure 3

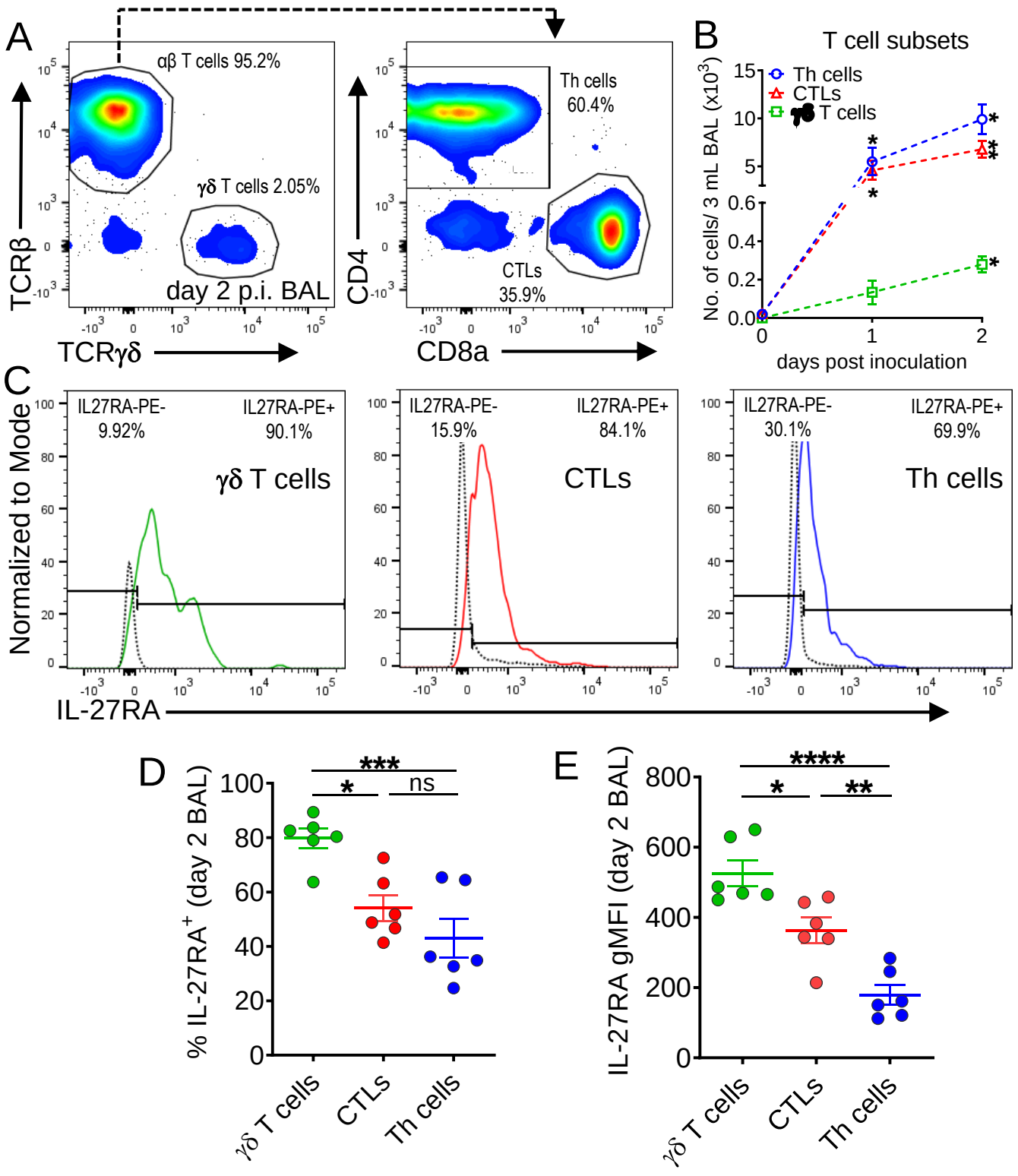
A
αβ T cells 95.2%
γδ T cells 2.05%
day 2 p.i. BAL
TCRβ
TCRγδ
Th cells
60.4%
CTLs
35.9%
CD4
CD8a
B
T cell subsets
Th cells
CTLs
γδ T cells
No. of cells/ 3 mL BAL (x10^3)
days post inoculation
C
Normalized to Mode
IL27RA-PE-
9.92%
IL27RA-PE+
90.1%
γδ T cells
IL27RA-PE-
15.9%
IL27RA-PE+
84.1%
CTLs
IL27RA-PE-
30.1%
IL27RA-PE+
69.9%
Th cells
IL-27RA
D
% IL-27RA+ (day 2 BAL)
***
*
ns
γδ T cells
CTLs
Th cells
E
IL-27RA gMFI (day 2 BAL)
****
*
**
γδ T cells
CTLs
Th cells

Figure 4

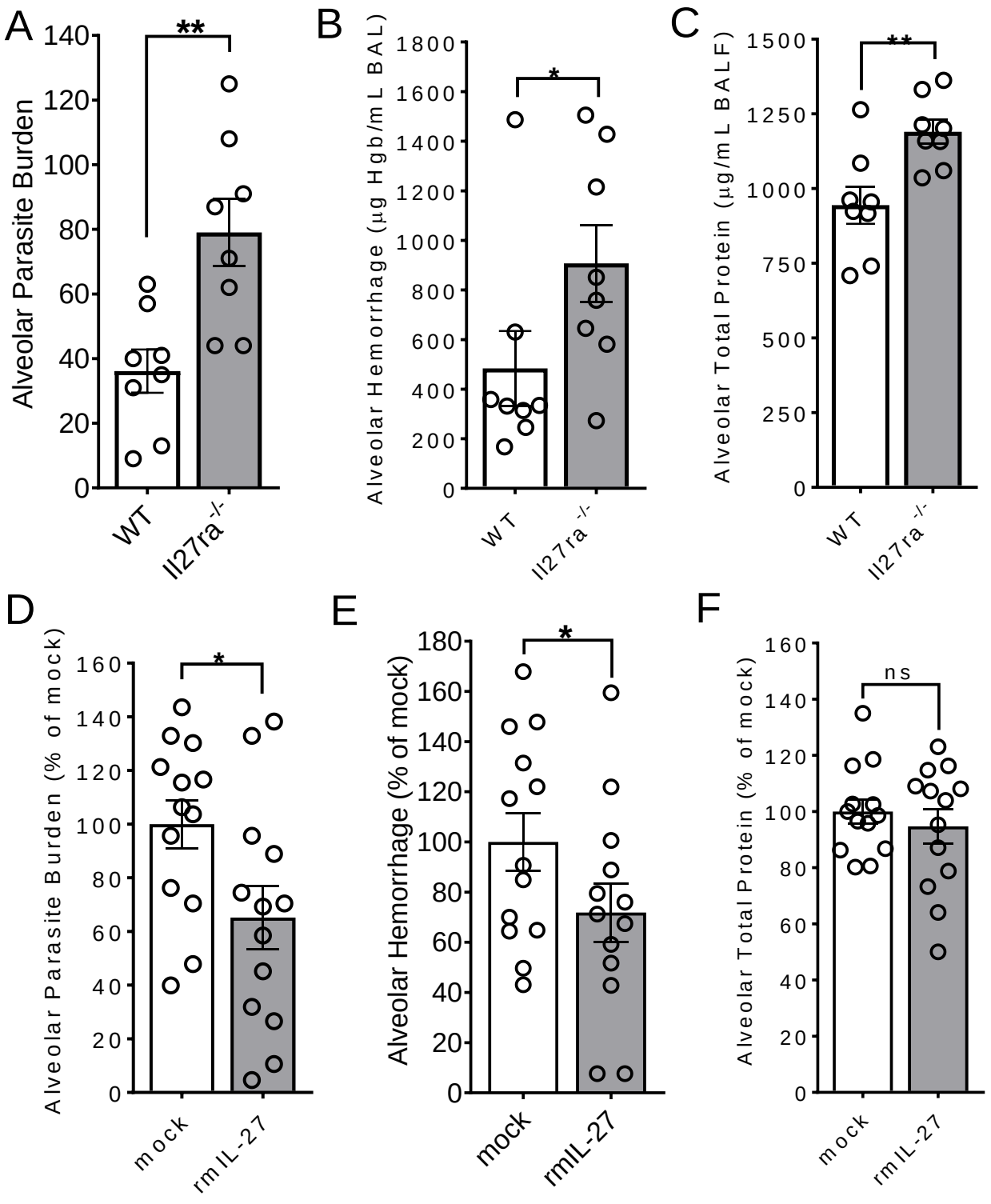
A
Alveolar Parasite Burden
140
120
100
80
60
40
20
0
**
WT
Il27ra-/-
B
Alveolar Hemorrhage (µg Hgb/mL BAL)
1800
1600
1400
1200
1000
800
600
400
200
0
*
WT
Il27ra-/-
C
Alveolar Total Protein (µg/mL BALF)
1500
1250
1000
750
500
250
0
**
WT
Il27ra-/-
D
Alveolar Parasite Burden (% of mock)
160
140
120
100
80
60
40
20
0
*
mock
rmIL-27
E
Alveolar Hemorrhage (% of mock)
180
160
140
120
100
80
60
40
20
0
*
mock
rmIL-27
F
Alveolar Total Protein (% of mock)
160
140
120
100
80
60
40
20
0
ns
mock
rmIL-27

Figure 5

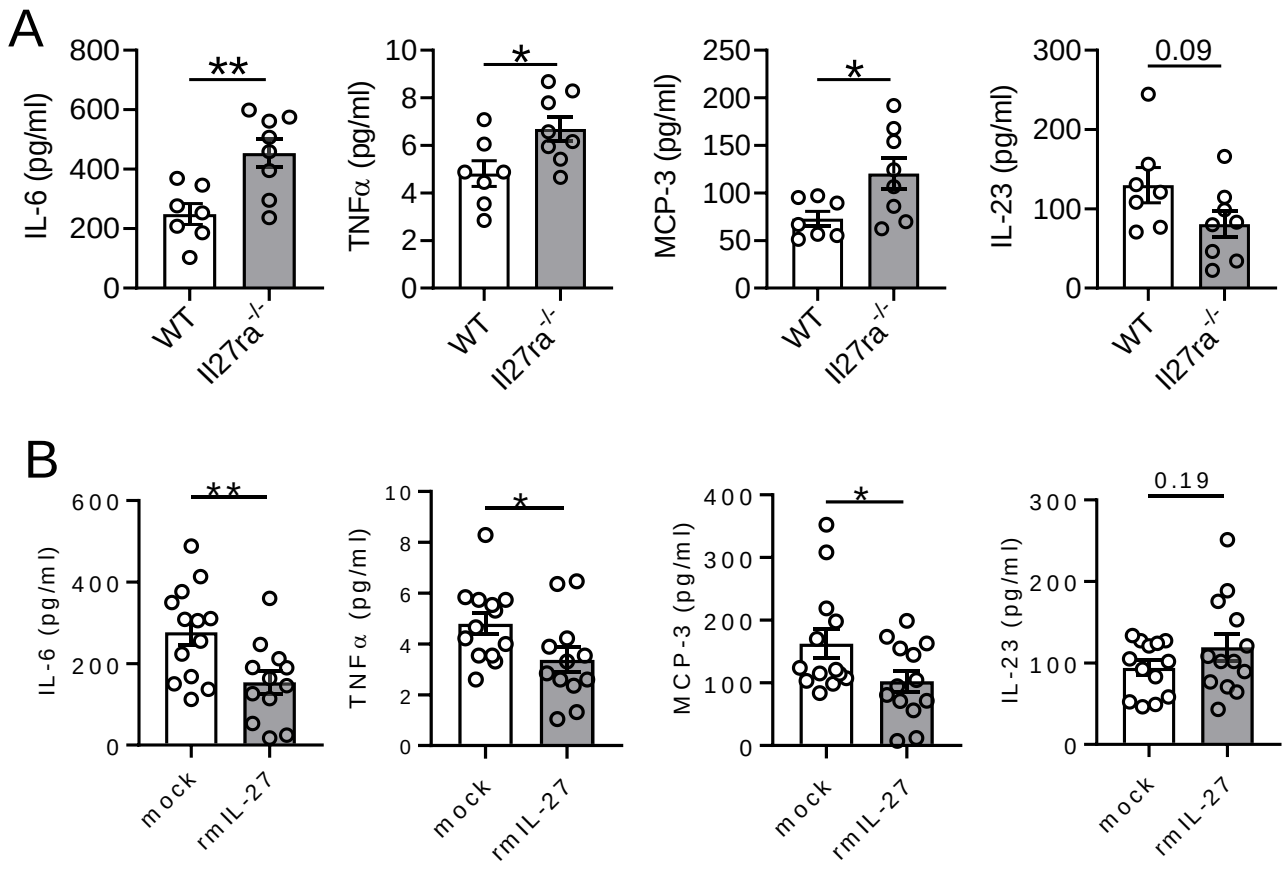
A
IL-6 (pg/ml)
800
600
400
200
0
**
WT
Il27ra-/-
TNFα (pg/ml)
10
8
6
4
2
0
*
WT
Il27ra-/-
MCP-3 (pg/ml)
250
200
150
100
50
0
*
WT
Il27ra-/-
IL-23 (pg/ml)
300
200
100
0
0.09
WT
Il27ra-/-
B
IL-6 (pg/ml)
600
400
200
0
**
mock
rmIL-27
TNFα (pg/ml)
10
8
6
4
2
0
*
mock
rmIL-27
MCP-3 (pg/ml)
400
300
200
100
0
*
mock
rmIL-27
IL-23 (pg/ml)
300
200
100
0
0.19
mock
rmIL-27

Figure 6

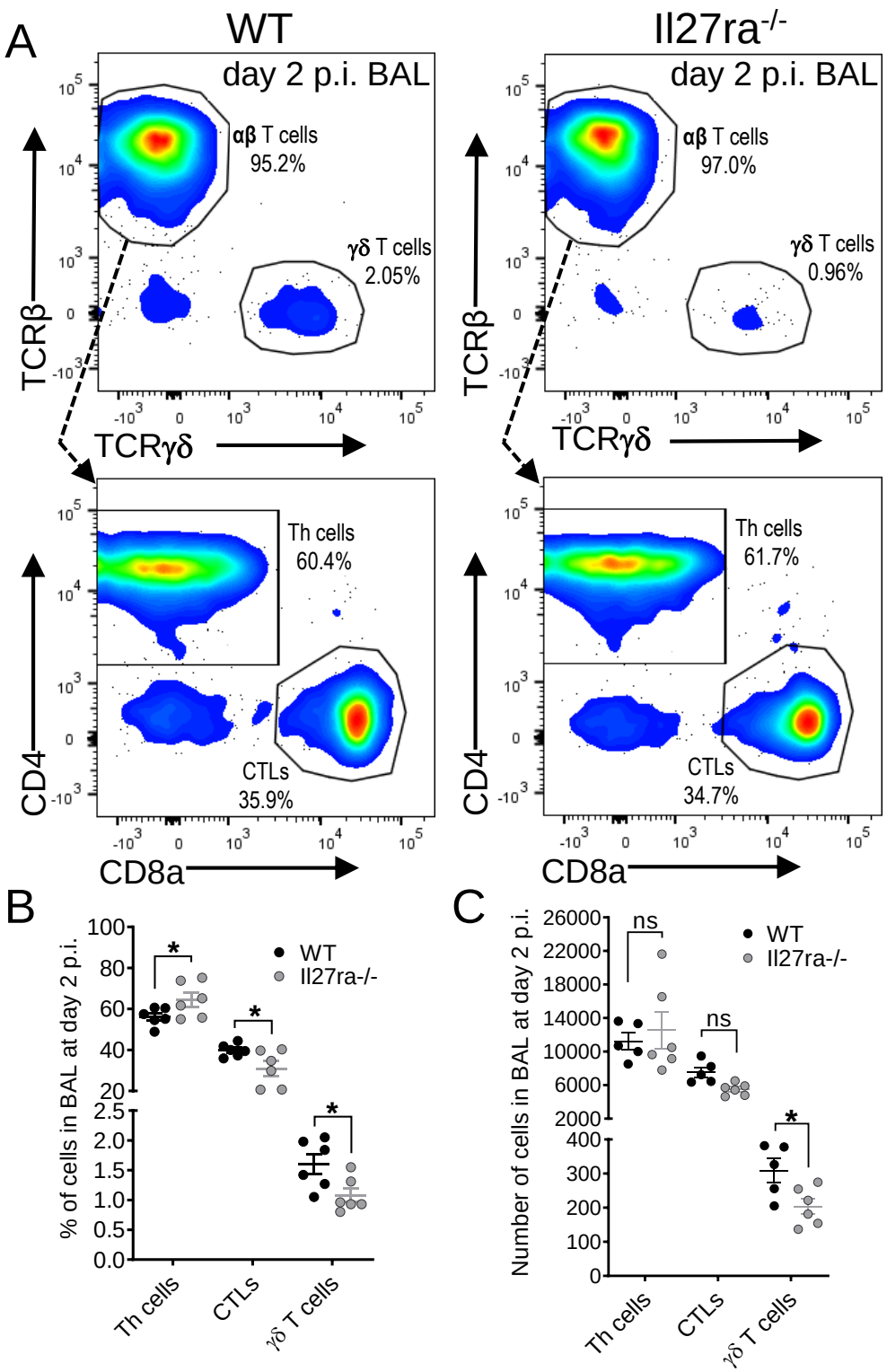
A
WT
Il27ra-/-
day 2 p.i. BAL
αβ T cells
95.2%
γδ T cells
2.05%
αβ T cells
97.0%
γδ T cells
0.96%
TCRβ
TCRγδ
Th cells
60.4%
CTLs
35.9%
Th cells
61.7%
CTLs
34.7%
CD4
CD8a
B
% of cells in BAL at day 2 p.i.
WT
Il27ra-/-
Th cells
CTLs
γδ T cells
C
Number of cells in BAL at day 2 p.i.
ns
ns
*

Supplemental Data

IL-27 enhances the lymphocyte mediated innate resistance to primary hookworm infection in the lungs

Jason B. Noon [§,*], Arjun Sharma[§, †, *], Johannes Platten[†], Lee J. Quinton[§], Christoph Reinhardt[†], and Markus Bosmann[§, †, ‡]

[§]Pulmonary Center, Department of Medicine, Boston University School of Medicine, Boston, Massachusetts, 02118, USA
[†]Center for Thrombosis and Hemostasis, University Medical Center of the Johannes Gutenberg University Mainz, 55131, Mainz, Germany
[‡]Research Center for Immunotherapy (FZI), University Medical Center of the Johannes Gutenberg-University Mainz, 55131, Mainz, Germany
[*]These authors contributed equally to the work.

Corresponding Author: Markus Bosmann, Associate Professor of Medicine, Pathology & Laboratory Medicine, Pulmonary Center, Department of Medicine, Boston University School of Medicine, Boston, Massachusetts, 02118, USA, Phone: +1-617-358-1225, FAX: +1-617-638-5227. E-mail: mbosmann@bu.edu

Figure S1

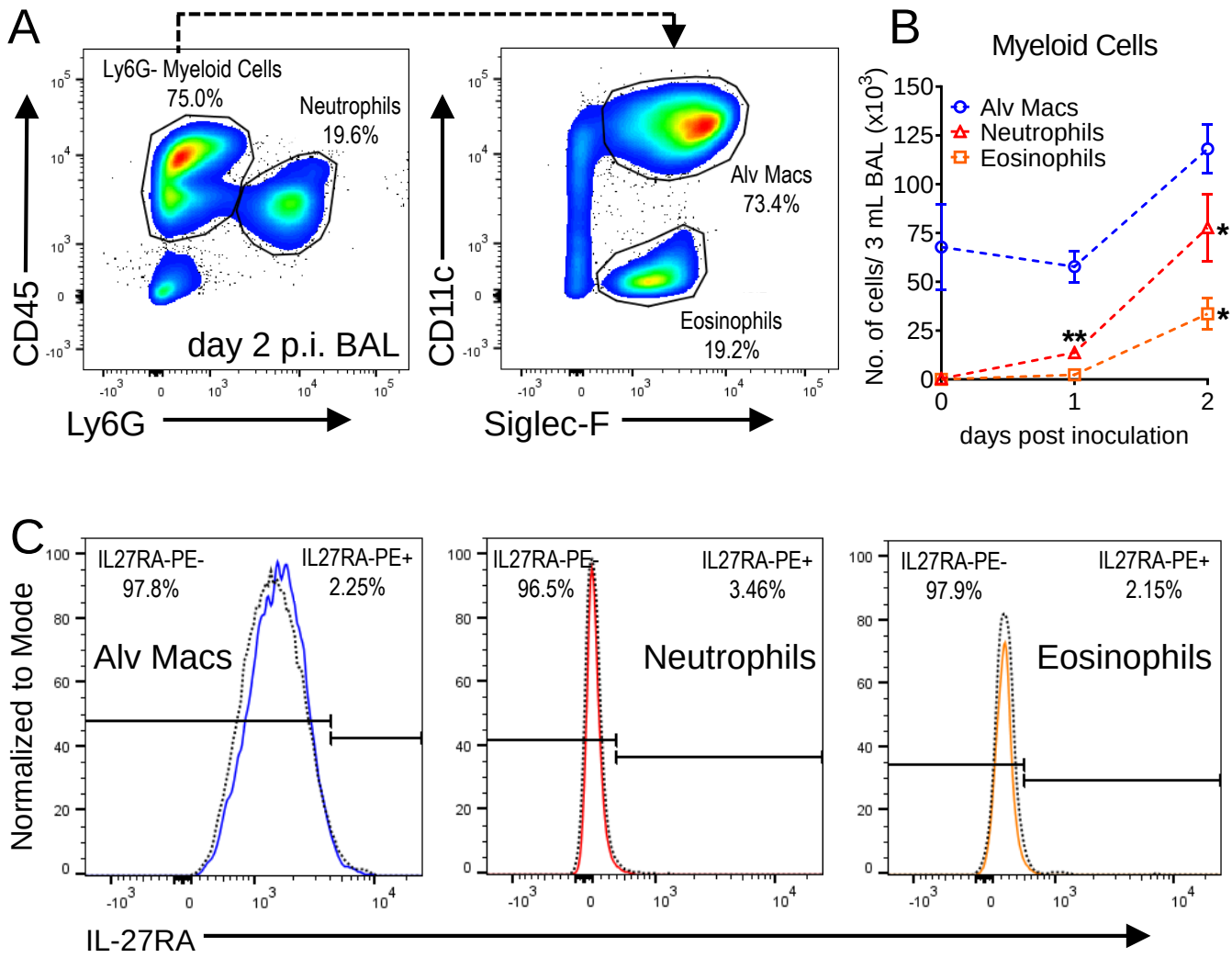

FIGURE S1. IL-27RA is not expressed on alveolar macrophages, neutrophils or eosinophils from the alveolar space during *N. brasiliensis* infection.

(**A**) Flow cytometry plots including gating strategy of CD45 versus Ly6G pre-gated on single myeloid cells (left) and CD11c versus Siglec-F on Ly6G$^-$ myeloid cells (right). Percentages are indicated next to each gate. (**B**) Numbers of Ly6G$^+$ neutrophils, Ly6G$^-$CD11c$^+$Siglec-F$^+$ alveolar macrophages and Ly6G$^-$CD11c$^-$Siglec-F$^+$ eosinophils on day 0 (PBS-inoculated/uninfected), day 1 and day 2 post-inoculation (n=3 mice/group) in BAL; day 0 vs. day 1 and day 0 vs. day 2 using two-tailed t-test, data shows mean ± SEM. (**C**) Histograms of IL-27RA expression on Ly6G$^-$CD11c$^+$Siglec-F$^+$ alveolar macrophages (left), Ly6G$^+$ neutrophils (middle) and Ly6G$^-$CD11c$^-$Siglec-F$^+$ eosinophils (right) on day 2 p.i. The dotted line indicates isotype-FMO control. The percentages of IL-27RA$^-$ and IL-27RA$^+$ cells are indicated in the upper left and right corners, respectively.

Figure S2

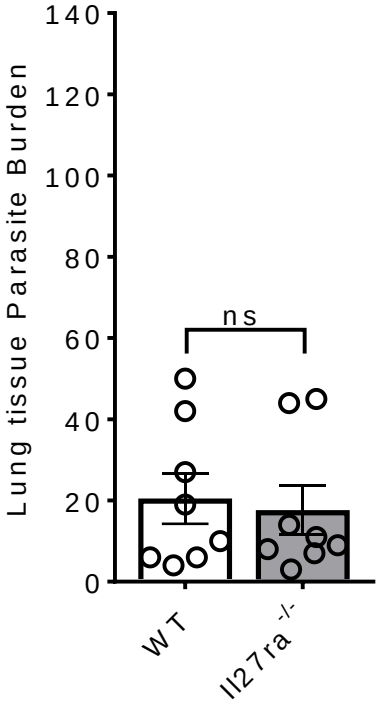

FIGURE S2. Parasite burdens are similar between wild type mice compared to Il27ra$^{-/-}$ mice in the lung tissues during *N. brasiliensis* infection.

Wild type mice (C57BL/6NJ) and Il27ra$^{-/-}$ mice were inoculated s.c. with L3 larvae (n=500/mouse). Parasite numbers were counted in whole lung tissues after removal of intra-airway parasites by multiple BAL on day 2 of infection. Lungs were minced from the same experiments as shown in Fig. 4A. Comparison of mean ± SEM analyzed by two-tailed t-test and each circle indicates the value of an individual mouse, ns: not significant.

Figure S3

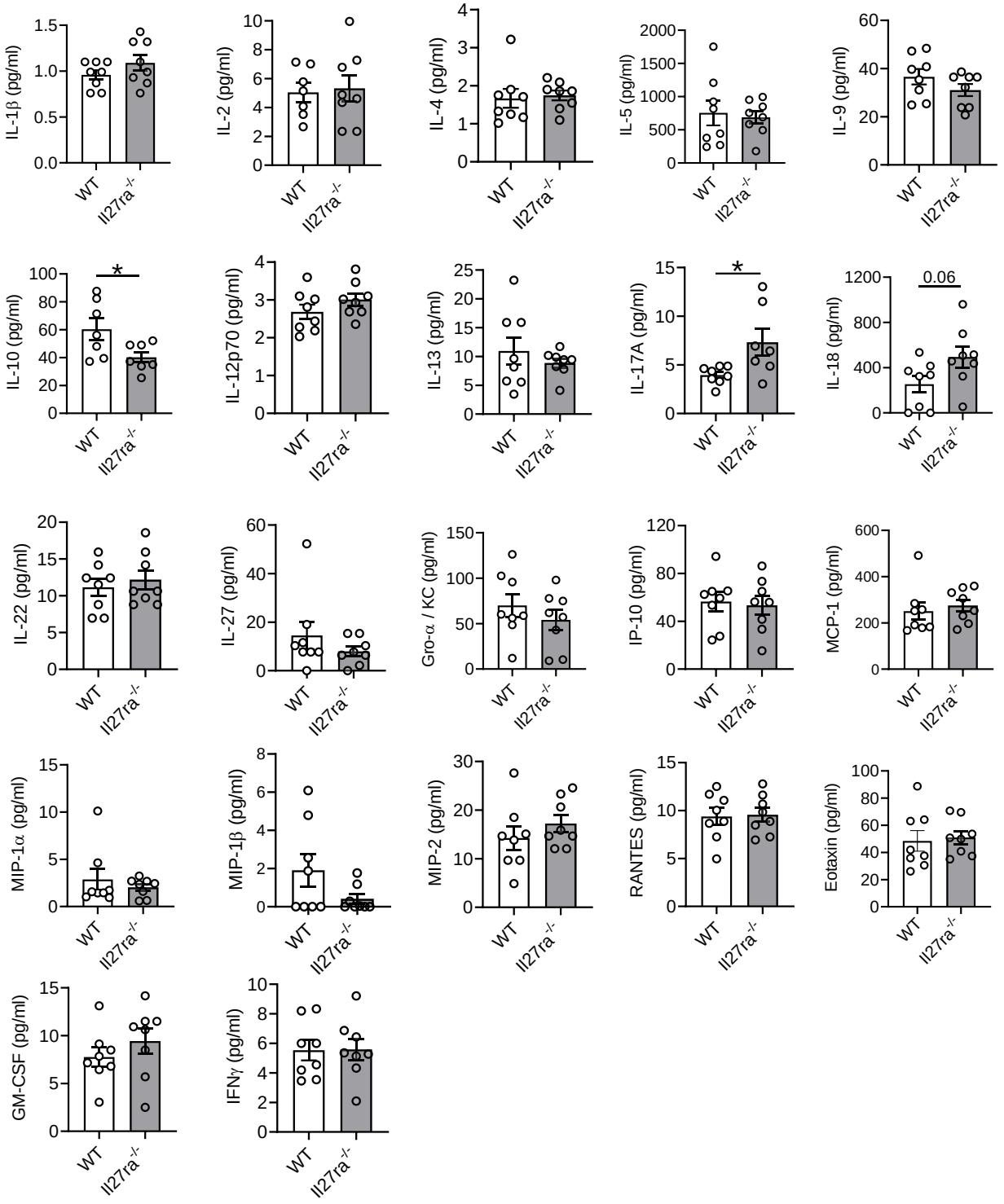

FIGURE S3. Cytokines and chemokines in brochoalveolar lavage fluids of Il27ra$^{-/-}$ mice.
In vivo comparison of different cytokines and chemokines of Il27ra$^{-/-}$ mice and wild type (WT; C57BL/6NJ) mice during primary *N. brasiliensis* infection (L3 n=500/mouse) in BALF after 2 days, bead-based multiplex assay. Data are shown as mean ± SEM and each circle represents an individual mouse, two-tailed t-test, * P<0.05, ** P<0.01.

Figure S4

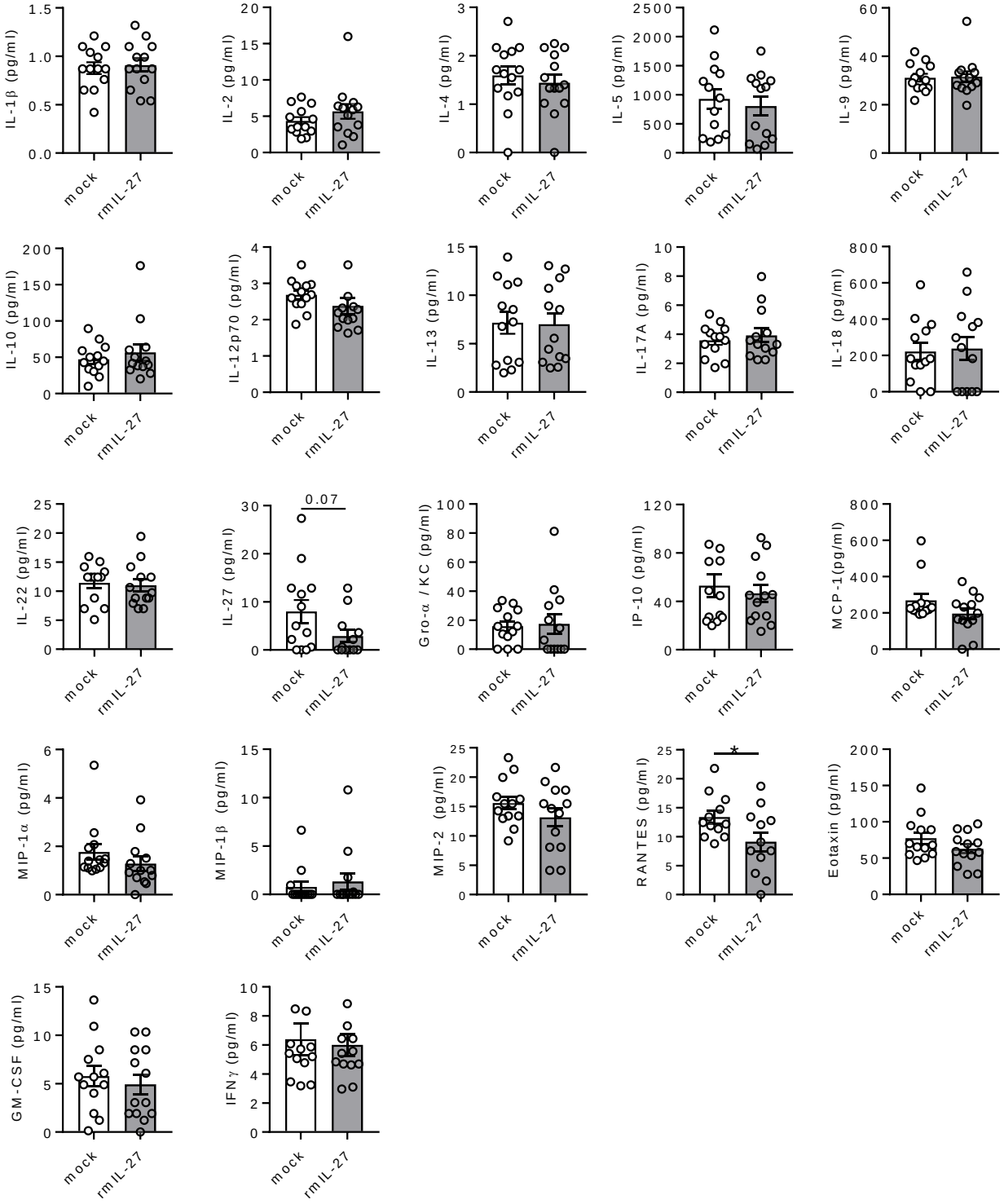

FIGURE S4. Cytokines and chemokines in brochoalveolar lavage fluids after treatment with recombinant mouse IL-27.

In vivo comparison of mediators in BALF from WT mice (C57BL/6J) administered with rmIL-27 (100 ng/mouse i.p.) or mock control (0.1% BSA in PBS) on day 0 and day 1 of *N. brasiliensis* infection and analyzed after 2 days p.i. Data are shown as mean ± SEM and each circle indicates an individual mouse, two-tailed t-test, * $P<0.05$.